Review

ATP synthase: from single molecule to human bioenergetics

By Yasuo KAGAWA[*1,*2,†]

(Communicated by Fumio OOSAWA, M.J.A.)

Abstract: ATP synthase (F_oF_1) consists of an ATP-driven motor (F_1) and a H^+-driven motor (F_o), which rotate in opposite directions. F_oF_1 reconstituted into a lipid membrane is capable of ATP synthesis driven by H^+ flux. As the basic structures of F_1 ($\alpha_3\beta_3\gamma\delta\varepsilon$) and F_o (ab_2c_{10}) are ubiquitous, stable thermophilic F_oF_1 (TF_oF_1) has been used to elucidate molecular mechanisms, while human F_1F_o (HF_1F_o) has been used to study biomedical significance. Among F_1s, only thermophilic F_1 (TF_1) can be analyzed simultaneously by reconstitution, crystallography, mutagenesis and nanotechnology for torque-driven ATP synthesis using elastic coupling mechanisms. In contrast to the single operon of TF_oF_1, HF_oF_1 is encoded by both nuclear DNA with introns and mitochondrial DNA. The regulatory mechanism, tissue specificity and physiopathology of HF_oF_1 were elucidated by proteomics, RNA interference, cytoplasts and transgenic mice. The ATP synthesized daily by HF_oF_1 is in the order of tens of kilograms, and is primarily controlled by the brain in response to fluctuations in activity.

Keywords: F_oF_1, molecular motor, mitochondria, omics, cytoplasts, bioenergetics

Introduction

All human activity depends on ATP, which is primarily synthesized *via* mitochondrial oxidative phosphorylation (oxphos). By analogy with glycolytic ATP synthesis, there have been many futile attempts to isolate hypothetical high-energy intermediates, such as phosphoenolpyruvate, that tightly couple respiratory energy to ATP synthesis. In 1961, Mitchell proposed the chemiosmotic hypothesis, which states that in oxphos, the respiratory energy is coupled to an imaginary anisotropic "ATPase system" located in an ion-impermeable membrane (Fig. 1 of Ref. 1) *via* H^+/OH^- flux driven by the electrochemical activity ($[H^+]_{Left}/[H^+]_{Right} = 10^7 \times [ATP]/[ADP]$) across the membrane.[1)] At the same time, soluble ATPase, known as coupling factor 1 (F_1), was purified from mitochondria in Racker's laboratory.[2)] When F_1 was bound to F_1-deficient mitochondrial membrane, respiratory energy was coupled to ATP synthesis.[2)] The author then isolated the entire ATP synthase, later called F_oF_1 (Fig. 1, right), and reconstituted F_oF_1 into liposomes capable of converting energy from ATP hydrolysis to that for H^+ flux driven by the electrochemical potential of protons across the membrane ($\Delta\mu H^+$), where $\Delta\mu H^+ = F\Delta\psi - 2.3RT\Delta pH$.[3)] The H^+ flux through

[*1] Department of Biochemistry, Jichi Medical School, Tochigi, Japan.
[*2] Department of Medical Chemistry, Kagawa Nutrition University, Saitama, Japan.
[†] Correspondence should be addressed: Y. Kagawa, Department of Medical Chemistry, Kagawa Nutrition University, 3-9-21 Chiyoda, Sakado, Saitama 350-0288, Japan (e-mail: kagawa@eiyo.ac.jp).

Abbreviations: AMPPNP, 5′-adenylyl-imindo diphosphate; ANC, Adenine nucleotide carrier; α, β, γ, δ and ε, subunits of F_1; β_E, β_D, and β_T, β subunit of F_1 with an empty catalytic site, with bound ADP or with bound ATP, respectively; a, b, c, d, e, f and g, A6L, subunits of F_o; c_{10}, decamer ring of the c subunit of F_o; F_oF_1, ATP synthase; F_1, ATP-driven motor of F_oF_1; F_o, H^+-driven motor of F_oF_1; BF_1, CF_1, EF_1, HF_1, TF_1 and YF_1, F_1 from bovine mitochondria, chloroplasts, *E. coli*, human mitochondria, thermophilic bacillus PS3 and yeast, respectively; $\Delta\psi$, membrane potential; $\Delta\mu H^+$, electrochemical potential difference of protons across the membrane; F, Faraday constant; FRET, florescence resonance energy transfer; IF, F_1 inhibitor; mtDNA, mitochondrial DNA; nDNA, nuclear DNA; OPA-1, optic atrophy 1; Oxphos, oxidative phosphorylation; Pi, inorganic phosphate; PIC, Phosphate carrier; P-loop, -G-X-X-X-X-G-K-T- sequence of the α and β subunits of F_1; R, gas constant; VDAC, voltage-dependent anion channel. For nomenclature of the amino acid residues in subunits α, β, γ, *etc.*, of F_1, "βK35", for example, refers to a lysine (K) residue located at #35 in the β subunit of F_1. The equivalent residues in different F_1s are expressed as thermophilic βK164 (=human βK162). Mutations are abbreviated as "βK164I", which means "residue K164 in the β subunit is changed to I164".

doi: 10.2183/pjab.86.667

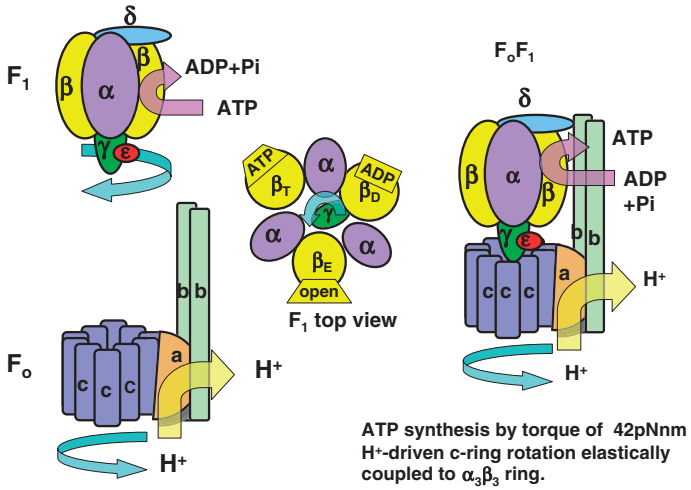

Fig. 1. Basic structure of TF_1 (ATP-driven motor), TF_o (proton-driven motor) and TF_oF_1 (proton-driven ATP synthase). Upper left: Side view of TF_1 composed of α, β, γ, δ, and ε subunits. The $\gamma\varepsilon$ turns counterclockwise against the $\alpha_3\beta_3$ hexamer in the ATP hydrolysis direction when viewed from the F_o side. Middle: Top view of TF_1 with three different conformations of β subunits. Lower left: Side view of TF_o composed of a, b and c subunits. The c_{10} ring turns clockwise against ab_2 in the proton-driven direction. Right: Side view of TF_oF_1. The central stalk ($\gamma\varepsilon$) turns with the c_{10} rotor clockwise in the ATP synthesis direction when viewed from TF_o side.

F_oF_1 liposomes was demonstrated first by a pH meter (Fig. 6 of Ref. 3). After the primary chemiosmotic hypothesis[1] was thus partially established,[3] the subunit-subunit interactions in F_oF_1 during ATP synthesis became the next research target. Boyer proposed a hypothetical two-subunit model of conformational energy transfer, and finally proposed the rotational hypothesis in 1981,[4] based on our report on thermophilic F_1 (TF_1) subunits with ubiquitous stoichiometry $\alpha_3\beta_3\gamma\delta\varepsilon$ (Fig. 1, upper left)[5] and conformational changes of isolated $TF_1\beta$ from β_E (with an empty catalytic site) to β_D or β_T by binding ADP or ATP, respectively.[6),7]

The objectives of this review are to publish how achievements on thermophilic F_oF_1 (TF_oF_1) in Japan have advanced the primary chemiosmotic[1] and rotational[4] theories, and how our studies on human F_oF_1 (HF_oF_1) will contribute to the development of human bioenergetics. To date, ligand-binding α or β subunits have only been isolated and reconstituted into $\alpha\beta$ subcomplexes from TF_1.[5)–7] In contrast to active $\alpha_3\beta_3$ hexamer and $\alpha_1\beta_1$ dimer of TF_1,[7] attempts to reconstitute $\alpha\beta$ subcomplexes from *E. coli* F_1 (EF_1) and HF_1 *in vitro* has been unsuccessful. However, functional complementation of yeast F_1 (YF_1) in a quintuple deletion mutant ($\Delta\alpha\Delta\beta\Delta\gamma\Delta\delta\Delta\varepsilon$) with genes encoding α, β, γ and ε of BF_1 strongly suggests the presence of common structure and function of HF_1 subunits.[8] Thus, the molecular mechanisms by which rotation and catalysis are coupled were mainly elucidated by crucial experiments using TF_1 and TF_o (ab_2c_{10}) to represent all F_oF_1s.[7] The rotational hypothesis[4] assumes that on ATP synthesis, the eccentric central stalk ($\gamma\varepsilon$) connected to the c_{10} ring is rotated against the $\alpha_3\beta_3$ hexamer in the clockwise direction, as viewed from the F_o side (Fig. 1, right). This rotation induces cyclic conformational changes of β in the order of $\beta_E\rightarrow\beta_D\rightarrow\beta_T\rightarrow\beta_E$ so as to change the affinity for nucleotides, and finally release ATP to return to β_E (Fig. 1, middle and upper right).[4),7] In fact, Walker's X-ray crystallography of most of $\alpha_3\beta_3\gamma$ of BF_1 visualized the distinct conformations of β with different nucleotide occupancies (β_E, β_D and β_T).[9]

The concept of F_oF_1 as an H^+-driven rotor (γ-c_{10}) and stator (δ-ab_2), rotating with a torque of 42 pN nm, was predicted in 1996 (Fig. 1, right).[10] The most convincing evidence of the rotational hypothesis was the direct observation of the rotation of an actin filament attached to γ against the fixed $\alpha_3\beta_3$ hexamer by Noji[11] in 1997, using the TF_1 gene.[12] Briefly, the ATP-driven F_1 motor rotates clockwise (Fig. 1, upper left) and the H^+-driven F_o motor rotates in the anticlockwise direction as viewed from the F_1 side (Fig. 1, lower left).[7),10),11] Preliminary experiments on "the 120° rotation of the c subunit oligomer" have been reported,[13] but this was not sensitive to F_o inhibitor and may represent the γ

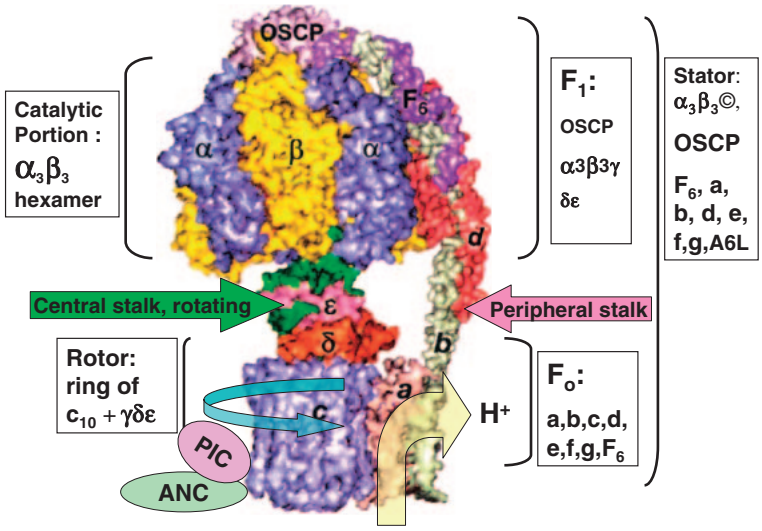

Fig. 2. Side view of space filling model of HF_oF_1. As there is high homology among F_oF_1s from different species,[12),17)–21)] and quintuple yeast deletion YF_1 mutant ($\Delta\alpha\Delta\beta\Delta\gamma\Delta\delta\Delta\varepsilon$) is complemented by genes encoding BF_1,[8)] the major structure of eukaryotic F_oF_1 is apparently universal.[9),14),25),29),73)–76)] Thus, X-ray crystallography data for F_oF_1 subunits from different species were taken from RCSB Protein Data Bank (http://www.rcsb.org/pdb/results/results.do?outformat) and assembled according to sequence data for HF_oF_1.[21)] No high-resolution structural data are available for subunit a and the hinge region of subunit b. ATP synthasome contains both PIC and ANC.[31)] PIC: Phosphate carrier; ANC: Adenine nucleotide carrier.

rotation in the F_1 portion of F_oF_1. In fact, crystallographic analysis of yeast F_oF_1 (YF_oF_1) revealed that the ring of c subunits contains 10 protomers, rather than the widely anticipated 12 ($4H^+$ per 120° rotation), and tightly connected to $\gamma\delta\varepsilon$ complex.[14)] Although crystal of EF_o is not available, exact experiments on TF_oF_1 confirmed the c_{10}-ring structure (Fig. 1, right).[15)] By using single-molecule FRET measuring the change in the distance between the subunits a and c during the rotation (see section 6.1), a 36° sequential stepping mode of the c_{10}-ring rotation in F_oF_1 was confirmed.[16)] ATP is synthesized at the clefts between α and β by $\Delta\mu H^+$-driven H^+ flux when both motors are connected by central ($\gamma\varepsilon$) and peripheral stalks ($ab_2\delta$) to the c_{10}-ring in TF_1 (Fig. 1).[7),14),17)] Elucidation of primary structures of *E. coli* F_oF_1 (EF_oF_1)[18)] and TF_oF_1,[12),19)] and site-directed mutagenesis[18),20)] and suppression of the lost functions[18)] led to refinements in the rotational hypothesis including elastic power transmission.[10)]

After the primary rotational hypothesis[4)] was thus partially established,[7),10),11),17)] research on F_oF_1 was divided into single molecular elucidation of energy transduction at the atomic level using stable TF_oF_1[12),17),20)] and biomedical elucidation of human F_oF_1 (HF_oF_1)[21)] at the mitochondrial[22)] and *in vivo* levels.[23)] In contrast to the single operon of bacterial F_oF_1,[12),18),19)] animal F_oF_1 is encoded by both nuclear DNA[21),24),25)] and mitochondrial DNA.[22),26)] The primary structures of bovine F_oF_1 (BF_oF_1)[24),25)] and HF_oF_1[21),27),28)] were sequenced, and cDNAs of the β subunits of BF_1 and HF_1, for example, were found to share 99% amino acid homology and 94% nucleotide homology (authors report in 1986 quoted in Ref. 21). Although the core structure of TF_oF_1 ($\alpha_3\beta_3\gamma\delta\varepsilon + ab_2c_{10}$)[7),10),12)] (Fig. 1) was conserved in $H(B)F_oF_1$, it is more complex due to additional 8 subunits (d, e, f, g, A6L (ATP8), OSCP and F_6, plus a natural inhibitor called IF_1) (Fig. 2)[21),24),25)]; subunits δ and ε of TF_1 correspond to OSCP (oligomycin sensitivity conferring protein) and the $\delta\varepsilon$ complex in HF_1, respectively.[21)] Although mammalian δ subunit is partially homologous to ε subunit of TF_1, X-ray crystallographic data of both BF_1[29)] and YF_1[14)] showed that $\delta\varepsilon$ complex interacts with a Rossmann fold in the γ subunit, forming a foot and c_{10}-γ-δ-ε rotates as an ensemble central stalk (Fig. 2),[14),29)] similar to the ε subunit at the γ subunit in TF_1 (Fig. 1).[7),17)] In fact, the $\delta\varepsilon$ complex was dissociated from BF_1 by guanidine treatment as a stable heterodimer (Papageorgiou, S., and Solaini, G., 2004, PubMed abstract). So called minor subunits (e, f, g and A6L) of HF_o are unlikely to have a role directly in ATP synthesis, but they appear to influence oligomeric state of HF_oF_1.[21),25)] Supramolecular structures of HF_oF_1 include HF_oF_1 dimer[30)]

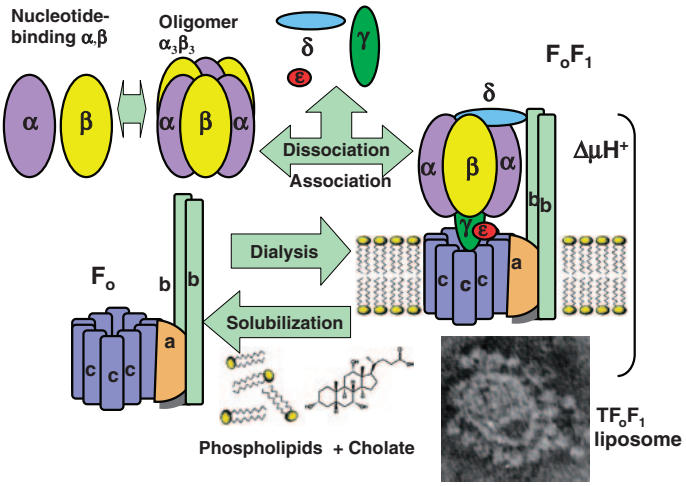

Fig. 3. Reconstitution of F_oF_1 from subunits and F_oF_1 liposomes from phospholipids.[3),39)] Isolated nucleotide-binding α and β subunits[6),56)] and $\alpha_3\beta_3$ hexamer were obtained by dissociation of TF_1 (upper left). Solubilized F_o or F_oF_1 was mixed with phospholipids and cholate, and dialyzed to reconstitute F_oF_1 liposomes (bottom right, electron micrograph) capable of proton-driven ATP synthesis.

and ATP synthasome[31)] composed of phosphate carrier (PIC), adenine nucleotide carrier (ANC) and HF_oF_1 (Fig. 2). Moreover, there are tissue differences in HF_oF_1, with muscle- and liver-type γ subunits in HF_1.[27)] The complex gene structure,[21),28)] specific regulation systems,[21),28)] expression and alternative splicing[27),32)] of HF_oF_1 and related regulatory genes were elucidated by recent cytoplast technology,[22),33)] transgenic mice,[32)] transcriptomics[21),32)] and proteomics.[31),32)] Based on the knowledge from these extensive studies,[7),17),21)] human energetics in physiological activities[21)] and diseases[21),23)] have been analyzed.

In this article, mechanistic studies of F_oF_1, including a reconstitution study and crystallography, will be reviewed, and then, more complex mitochondrial cytobiology and human biomedical studies will be described, because mitochondrial structure, neurohormonal control, tissue-specific activity and disease are not found in bacteria. Historical evaluations of contributions made by scientists in mechanistic studies are summarized in excellent reviews (Refs. 4 and 17, and references therein).

1. Isolation of ATP synthase (F_oF_1) by membrane biology

F_oF_1 is a membrane protein of oxidative phosphorylation. In the 1960s, membrane biology was in its infancy, and the many attempts to purify ATP-synthesizing membrane proteins from mitochondria had been unsuccessful. Long before Fleischer's group extracted phospholipids from the mitochondrial membrane with aqueous-acetone (10% water) and restored electron transport activity by adding back phospholipid micelles in 1962,[34)] Kakiuchi succeeded in a similar experiment in 1926.[35)] Okunuki[36)] succeeded in preparing several cytochromes. Green's group prepared electron transport components from mitochondria.[37)] However, even after phospholipids were added back and electron transport activity was restored,[34)–37)] liposomes capable of $\Delta\mu H^+$-driven oxphos, as predicted by Mitchell,[1)] were not reconstituted.

Membrane proteins were classified into extrinsic and intrinsic proteins.[3)] Extrinsic proteins, such as cytochrome c[36)] and F_1,[2),5)] or components of F_1, including OSCP[3),25)] and F_6[3),25)] (Figs. 1 and 2), are easily detached from the biomembrane by treatment with ultrasonic irradiation, chelating agents, and chaotropic anions (KI, KCN),[3)] and can be purified as soluble proteins in the water phase by chromatography and ammonium sulfate fractionation. However, intrinsic proteins including cytochrome oxidase[36),37)] and F_o[3)] are hydrophobic and embedded in the lipid bilayer, and require proper detergents for solubilization[3)] (Fig. 3, right). In 1966, detailed phase diagrams of phospholipid cholate system were reported,[38)] and these were useful for solubilizing intrinsic proteins and reconstituting functional biomembrane.[3),39),40)] The detergent concentration needed to solubilize F_oF_1 is near its critical micelle concentration.[3)]

The F_1 reported by Racker's laboratory[2] was not sensitive to an energy transfer inhibitor of oxphos, oligomycin, but became oligomycin sensitive when bound to F_1-depleted mitochondrial membrane.[41] The oligomycin sensitivity conferring factor (F_o, H^+-driven motor, Fig. 1) was characterized as an intrinsic membrane protein,[41] and by using cholate, oligomycin-sensitive ATPase, later designated F_oF_1, was isolated (Fig. 3).[3),42] F_oF_1 was reconstituted from F_o and F_1.[42] The electron microscopic images of BF_oF_1 revealed spherical ^{3}H-acetyl-BF_1 attached to membrane-embedded BF_o.[43] In combined morphological-biochemical studies to identify the *in situ* structure of BF_oF_1,[43] radiolabeled BF_1 was added to BF_o membrane, and then the structure, radioactivity and ATPase activity were removed in parallel.[43] However, mitochondrial F_1s, including BF_1 and HF_1, are unstable and reconstitution of F_1 from each isolated subunit was unsuccessful, even with chaperones. Thus, TF_1[7),44] and TF_oF_1[7),45] were purified from thermophilic bacillus PS3, and stable TF_oF_1 was reconstituted from TF_1 and TF_o (Fig. 1).[7),44),45] Recent proteomics using mild detergent extraction of HF_oF_1 from membrane followed by native gel electrophoresis revealed supramolecular structures including dimeric HF_oF_1[30] and ATP synthasome (PIC + ANC)[31] (Fig. 2) (see section 9).

2. Reconstitution of F_oF_1 membrane capable of ATP synthesis by proton flux

F_oF_1 converts energy of $\Delta\mu H^+$ driven H^+ flux into ATP synthesis. Incorporation of membrane proteins into the lipid bilayer is essential in activity studies in membrane biology. The most difficult step was the reconstitution of liposomes containing active membrane proteins capable of producing $\Delta\mu H^+$.[3),39),40] The use of removable detergents, including cholate, was essential in the preparation of BF_oF_1 (Fig. 3),[3),39),40] and after cholate extraction, Triton-X100 was used in the chromatography to purify TF_oF_1.[45] The removal of ^{14}C-cholate during dialysis was estimated by radioactivity,[3),40] and tight closure of the liposome membrane was estimated by radioactivity of enclosed ^{14}C-inulin and confirmed by electron microscopy of enclosed ferritin.[3),40] Electron microscopy showed liposomal membranes studded with closely neighboring F_1 (Fig. 3, lower right).[3),43] As several extrinsic proteins in oxphos, including F_1, OSCP and F_6 were partially lost during the extraction and dialysis of F_oF_1, the best activity was attained by adding these after dialysis.[3),39]

These liposomes showed H^+ translocation on addition of ATP,[3),40),46] ATP-^{32}Pi exchange reactions[3),39),46] or H^+-driven ATP synthesis (Fig. 1, right).[46] Thus, F_oF_1-liposome was shown to be the anisotropic "ATPase system" imagined by Mitchell.[1] ATP synthesis was sensitive to the combination of valinomycin (K^+ ionophore) and nigericin (H^+–K^+ exchange ionophore), which collapsed $\Delta\mu H^+$.[3),39),46]

More stable TF_oF_1-liposomes synthesized ATP from ADP and Pi with energy from proton flux driven by $\Delta\mu H^+$ formed by ΔpH and $\Delta\psi$ across their membranes.[46] Using chloroplasts, ATP synthesis from ADP and Pi was demonstrated by applying ΔpH using acid–base transition[47] and by imposing $\Delta\psi$ using an electric pulse.[48] However, chloroplasts contain an electron transport system and other components that are energized by either ΔpH or $\Delta\psi$. Thus, net ATP synthesis by applying ΔpH (acid–base transition) or $\Delta\psi$ (external electric pulse) to purified TF_oF_1 reconstituted in liposome[46] was the most convincing evidence of chemiosmotic theory.[1]

The electrical potential between the inside and outside of liposomes formed by K^+ diffusion in the presence of valinomycin was calculated as $\Delta\psi = RT/F \times \ln([K^+]_{out}/[K^+]_{in})$. Maximal net ATP synthesis from ADP and Pi was achieved by incubating vesicles in malonate at pH 5.5 with valinomycin, and then rapidly transferring them to a solution of pH 8.4 and 150 mM K^+.[7),46] To synthesize ATP, the minimal $\Delta\mu H^+$ ($= \Delta\psi - 60\Delta$pH, at 30°C) of 210 mV and optimal $\Delta\mu H^+$ of 290 mV was required.[46] The H^+-conducting activity of TF_o-liposome through TF_o was proportional to the imposed $\Delta\mu H^+$ ($6H^+$/sec/103 mV at pH 8.0).[49] The pH profile of the rate revealed that a proton, not a hydroxyl ion, was the true substrate.[49] Because of the kinetic equivalency between $\Delta\Psi$ and ΔpH as driving forces of ATP synthesis,[46] $\Delta\psi$ is expected to replace $\Delta\mu H^+$. In fact, TF_oF_1-liposomes irradiated with external electric pulses (760 V/cm, 30 ms, rectangular) catalyzed net ATP synthesis.[50] The amount of ATP synthesized increased with the number, voltage and duration of electric pulses.[50] The net synthesis of ATP by application of $\Delta\mu H^+$ across the TF_oF_1-liposomes[46),50] firmly established the chemiosmotic hypothesis.[1] To directly measure $\Delta\Psi$ with electrodes on both sides of the membrane, TF_oF_1 was reconstituted into planar phospholipid bilayers, and the magnitude of the electric current generated upon addition of ATP was shown to follow simple Michaelis–Menten type kinetics, and the Km was found to be 0.14 mM.[51] There was no apparent

dependence of Km on $\Delta\Psi$.[51] This observation indicates that $\Delta\mu H^+$ does not directly affect Km to release the ATP formed on TF_oF_1,[7),51] and opens the way for conformational energy transfer in ATP synthesis.

Since the success of the F_oF_1-liposome,[3),39),46] the reconstitution method has been used to analyze the activity of intrinsic proteins including channels, receptors and membrane proteins. Using the liposome method, the important outer membrane diffusion channel known as VDAC, (voltage-dependent anion channel) in mitochondrial transport was isolated in 1980 (see sections 9 and 10).[52]

3. Reconstitution of F_1 subunit complexes capable of ATP synthesis by torque

3.1. Core components of F_o are a, b, and c subunits and those of F_1 are α, β, γ, δ and ε. The structure of F_oF_1 is shown in Figs. 1 and 2.[7),9),12),18),53),54] Complete reconstitution of F_1 (370 kDa), after complete denaturation of all subunits into their primary structures with sodium dodecylsulfate and urea and refolding into tertiary structure,[53] from subunits α (55 kDa), β (52 kDa), γ (32 kDa), δ (20 kDa) and ε (14 kDa) was possible only in TF_1 (Fig. 3).[53] The intermediate core subunit complexes, $\alpha_1\beta_1$ dimer[55] and $\alpha_3\beta_3$ hexamer,[55] were also only obtained in TF_1, although the sequence homologies of core subunits were conserved in HF_1 (371 kDa).[21] Enzymology revealed that $\alpha_3\beta_3$ hexamer was an oligomer, while $\alpha_1\beta_1$ dimer was a protomer.[55] Owing to the stability of TF_1, the subcomplexes with chemically modified and mutated subunits were useful for nanotechnology.[7),17),54]

TF_o (148 kDa) is composed of a (30 kDa), b (17 kDa) and c (8 kDa) in a stoichiometric ratio of 1:2:10 (Figs. 1 and 3).[7),12),17] HF_o and BF_o contain, in addition to the common subunits a (also called ATP6; 25 kDa), b (25 kDa), and c (8 kDa), minor subunits d (19 kDa), e (8 kDa), f (10 kDa), g (11 kDa), F_6 (9 kDa) and A6L (also called ATP8; 8 kDa)[18),25),29] (Fig. 2). The single stalk BF_o obtained by urea-cholate treatment of BF_oF_1 was reconstituted with externally added ^{3}H-acetyl-F_1 and the additional peripheral stalk components OSCP and F_6 were demonstrated in 1971.[3),39),40] Isolated BF_o subunits other than OSCP and F_6 are unstable, and their reconstitution has been unsuccessful without presequence and organizing machinery, even with chaperones.[21] These BF_o subunits were only identified on gel electrophoresis and X-ray crystallography.[25),29] F_oF_1 was seen as a sphere ($\alpha_3\beta_3$ hexamer portion, diameter 12 nm× height 10 nm)[43] connected by two stalks (central and peripheral) to a basal piece (subunits a and c_{10} ring) (Fig. 3, lower right).[3),43]

3.2. Protomeric, oligomeric and rotational ATPases: $\alpha_1\beta_1$ dimer, $\alpha_3\beta_3$ hexamer and $\alpha_3\beta_3\gamma$ heptamer. The isolated α and β subunits of TF_1 both have AT(D)P-Mg binding activity accompanied by conformational changes[6] without ATPase activity (Fig. 3, left).[55),56] The open structure of β_E and closed structures of β_D and β_T in the presence of ligands were confirmed in the isolated thermophilic β using ^{1}H-NMR.[56] Both thermophilic α and β subunits were reconstituted to form an active $\alpha_1\beta_1$ dimer by forming a catalytic $\alpha\beta$ interface.[55] Three $\alpha_1\beta_1$ dimers were reconstituted to form an allosterically active $\alpha_3\beta_3$ hexamer (Fig. 3, upper middle).[55] Both the high catalytic activity and formation of F_1-bound ATP from ADP + Pi depend on the $\alpha_3\beta_3\gamma$ structure with rotational ATPase.[7),11),17] There are six potential nucleotide-binding sites on F_1 and $\alpha_3\beta_3\gamma$: three catalytic sites on β and three noncatalytic sites on α,[7),17] as confirmed by X-ray crystallography.[9]

Depending on the occupancy of catalytic sites with increasing ATP concentration ([ATP]), there are three types of ATPase activities of F_1: uni-site, bi-site and tri-site.[4),57] Uni-site catalysis is measured at sub-stoichiometric ATP concentrations ([ATP] < $[F_1]$). Uni-site activity is very low, and the apparent Km_{ATP} is less than 20 nM.[57] The ATPase activity of the $\alpha_1\beta_1$ dimer of TF_1[57] showed typical Michaelis–Menten kinetics with only one K_{mATP} value of 70 µM, and a Vmax value of 0.1 unit/mg, without the cooperative characteristics of a protomer.[57] In contrast, ATPase activity of the $\alpha_3\beta_3$ hexamer showed the cooperative characteristics of an oligomer.[58] The apparent Km_{ATPs} of oligomeric ATPase of $\alpha_3\beta_3$ at 25°C were about 150 µM (bi-site) and 490 µM (tri-site).[58] Km_{ATPs} of rotational ATPase of TF_1 (Fig. 3, right) were about 80 µM (bi-site) and 490 µM (tri-site).[58] The γ-containing complexes $\alpha_3\beta_3\gamma$, $\alpha_3\beta_3\gamma\delta$ and $\alpha_3\beta_3\gamma\varepsilon$, show common kinetic properties.[59] The $\alpha_3\beta_3$ hexamer was inhibited by only one mole of [^{3}H]-3′-O-(4-benzoyl) benzoyl-ADP per hexamer, similarly to both BF_1 and TF_1.[60] Thus, the presence of only one inhibited-β in the hexamer blocked multi-site steady-state ATPase activity. This single-hit inactivation and cooperativity is an inherent property of the symmetrical $\alpha_3\beta_3$, but is not the due to the inhibition of rotation by TF_1 or $\alpha_3\beta_3\gamma$.

3.3. Rotation of the γ subunit in $\alpha_3\beta_3$ hexamer of TF_1: One mole ATP hydrolysis at

one β subunit drives 120° rotation of γ subunit in a concerted manner. The rotational hypothesis of F_oF_1[4] was also proposed by Oosawa as the "loose coupling mechanism of rotational proton ATPase" based on analogy with the H^+-driven flagella motor in 1986.[61] The rotation of the γ subunit axis in the cylinder of the $\alpha_3\beta_3$ hexamer in the F_oF_1 motor with the torque of 42 pN nm was predicted by many lines of evidence.[10] The rotation of γ was directly demonstrated in single-molecule studies using $\alpha_3\beta_3\gamma$ from TF_1.[11] Rotational motion was visualized by attaching a fluorescently labeled actin filament (1–4 μm) to γS107C of artificially induced mutant γ subunit with the biotin-streptavidine bridge. The $\alpha_3\beta_3$ hexamer was immobilized on a glass surface of Ni-nitrilotriacetate by artificially attaching decapolyhistidine to β,[11] and the ATP-driven rotation of the γ subunit was found to be anticlockwise when F_1 was observed from the F_o side (Fig. 1, upper left).[11),17]

The work performed by the rotating γ in a fixed $\alpha_3\beta_3$ is the frictional torque times angle of rotation. The hydrodynamic frictional drag coefficient (ξ) of the actin filament for the propeller rotation is given by $\xi = (\pi/3)\eta L^3/[\ln(L/2r) - 0.447]$, where, η (10^{-3} N s m^{-2}) is the viscosity of the medium, L, the length of the actin filament (1–4 μm) and r, the radius of the filament (5 nm).[11] The observed rates of filament rotation at 2 mM ATP are 7, 1, and 0.1 revolutions per second, when the lengths of f-actin are 1, 2 and 4 μm, respectively.[11] The frictional torque $\xi\omega$ was about 40 pN nm, where ω is the angular velocity.[11] Hydrolysis of one ATP molecule drives a 120° rotation of the γ subunit relative to the cylinder of the $\alpha_3\beta_3$ hexamer, and therefore, hydrolysis of three ATP molecules is required for one complete 360° revolution.[15),62] In order to analyze rapid rotation by reducing the viscosity resistance of long actin filament, fluorescent gold beads (40 nm) were attached to γ. At nanomolar ATP concentrations, β_E waits until the next ATP molecule is bound, and the duration of the pause depends on the ATP concentration (ATP-waiting dwell time).[62] ATP binding to β_E is the power step that drives the 80° rotation of γ.[55] This rotation leads to simultaneous release of ADP from the catalytic site of β_D, and hydrolytic cleavage of ATP into ADP and Pi at β_T after a pause (catalytic dwell time), and a 40° rotation occurs to complete the 120° rotation.[62]

Using mutant β (E190D) of TF_1, in the same rotational experiments, the catalytic activity of each β subunit was shown to be coordinated with the other two β subunits to drive rotation of the β_E, β_D, and β_T cycle.[63] Hybrid F_1 containing one or two mutations with altered catalytic kinetics rotates in an asymmetric stepwise fashion with different dwell times. Analysis of the rotation revealed that for any given β subunit, the subunit binds ATP at 0°, cleaves ATP at approximately 200° and carries out a third catalytic event at approximately 320°. This demonstrates the concerted nature of the F_1 complex activity, where all three β subunits participate to drive each 120° rotation of the γ subunit with a 120° phase difference.[63]

3.4. Torque-driven ATP synthesis by TF_1. ATP is synthesized by mechanical energy applied on the γ subunit without proton flux. ATP synthesis driven by mechanical energy (Fig. 1) was directly shown by attaching a magnetic bead (diameter = 700 nm, biotinylated) to the γ subunit of $\alpha_3\beta_3\gamma$ of mutant TF_1 (C193α, H_{10}-β, and S107Cγ, I210Cγ) on a glass surface, and rotating the bead using electrical magnets.[64] After the ATP-driven rotation of the beads was confirmed, the magnet was turned on and several bursts of hundreds of revolutions at 10 Hz were imposed.[64] Anticlockwise forced rotation of the γ subunit by the magnetic beads resulted in the appearance of ATP in the medium, as detected by counting the photons emitted from the luciferase–luciferin reaction with a camera (Hamamatsu Photonics).[64] This shows that torque working at one particular point (γ) on a protein complex can influence a chemical reaction occurring at physically remote catalytic sites (β), driving the reaction far from equilibrium.[64]

4. Genes for TF_oF_1 and HF_oF_1: Single operon vs. nuclear and mitochondrial genes

Detailed genetic analysis and site-directed mutagenesis have been reported by Futai using *E. coli* F_oF_1 (EF_oF_1), as *E. coli* genetics are well understood.[18),65] The catalytic, structural and regulatory significance of an amino acid residue in EF_1 was elucidated by site-directed mutagenesis.[65] However, many crucial experiments, including the planar F_oF_1 bilayer[51] and torque-driven ATP synthesis,[64] have not been successful to date with EF_oF_1, due to its fragility. Thus, a special sequencing method for thermophilic genes was developed.[66] The structure of the TF_oF_1 operon (number of amino acid residues),[12),19] I(127)-a(210)- c(72)- b(163)- δ(163)- α(502)- γ(286)- β(473)- ε(132), was similar to that of the EF_oF_1 operon.[18),65]

Amino acid residues in the different α, β, and γ subunits from TF_1,[12),19] HF_1,[21),27),28] BF_1[24] and

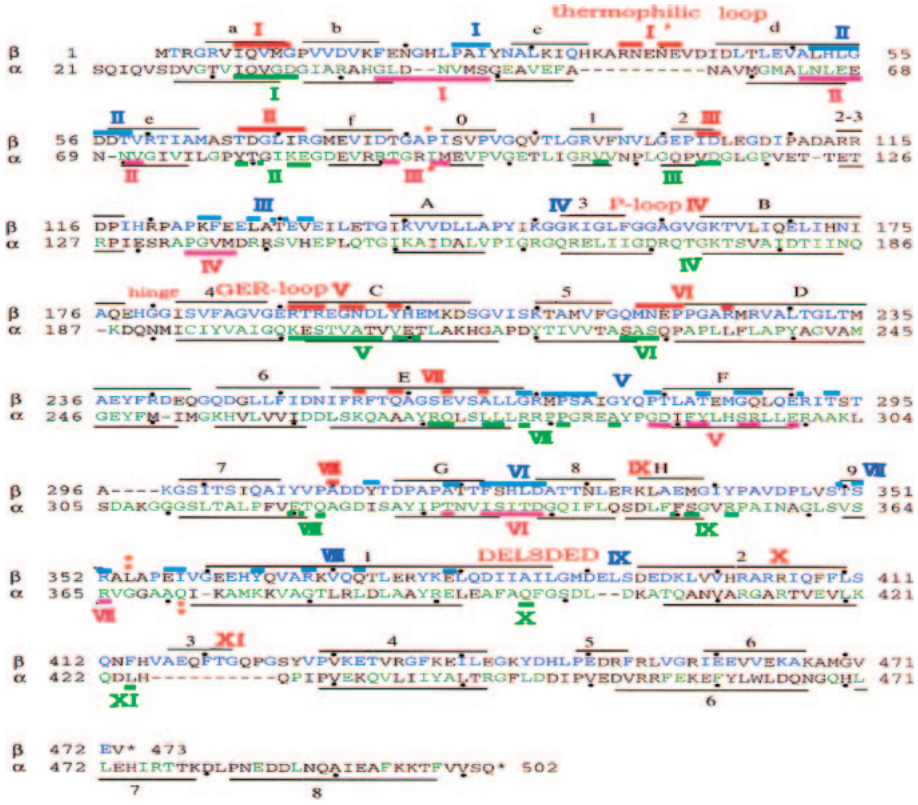

Fig. 4. Aligned amino acid sequences[12),19)] and secondary structure elements[71)] of α and β subunits in TF_1. Solid black lines indicate folds, and these were classified into α-helices (A–H, 1–8) and β-sheets (a–f, 0–8). The labels for folds are provided only for the β subunit, except for the three C-terminal α-helices in the α subunit. Dots indicate every tenth residue. I–XI: areas of $\alpha\beta$ contact. Red: catalytic contact areas of β. Pink: catalytic contact areas of α. Blue: non-catalytic contact areas of β. Green: non-catalytic contact areas of α. Colored bars indicate contact residues in $T\beta_E$. Sequences are divided by red asterisks (*) to indicate the three domains.

EF_1[18),65)] are aligned[19)] and expressed in the format α10, which refers to residue #10 in the α subunit. The residue numbers of amino acid sequences in the α and β subunits of TF_1 are shown in Fig. 4 (dots indicate every tenth residue).[17),19)] Primary structures are homologous, with 59% sequence identity between thermophilic α/human α and 68% between thermophilic β/human β.[19)] The primary structure of the TF_1 β subunit showed homology with 270 residues which are identical in the β subunits from HF_1, CF_1, and EF_1.[19)] The homologies of the amino acid sequence between BF_1 and YF_1 were 73%, 79% and 40%, respectively, for the α, β and γ subunits.[14)] As these YF_1 subunits were functionally complemented with corresponding BF_1 subunits,[8)] the essential structure is conserved among YF_1, BF_1 and HF_1 (sequence is nearly identical to that of BF_1, but there were polymorphisms in HF_1).[8)] Residues forming reverse turns (Gly and Pro) were highly conserved among the β subunits.[19)] Conserved residues (green and blue letters in Fig. 4) among TF_1, HF_1 and EF_1 are closely related to catalytic and regulatory functions.[19),21),65)] The observed substitutions in the thermophilic subunit increased its propensities to form secondary structures, and its external polarity to form tertiary structure.[19)]

Chemical and genetic modification of residues in F_1 revealed a nucleotide-binding P-loop (-GGAGVGKT-; thermophilic β158–165 corresponds to bovine β156–163) (Figs. 4, 5A).[7),9),12),19),54)] Long before the X-ray crystallographic elucidation of the P-loop,[9)] site-directed mutagenesis of the TF_1 gene[20)] to induce thermophilic βK164I and thermophilic αK175I, identified an essential role for lysine residues in the catalysis (Fig. 5A, red letters).[20)] The proton abstracting thermophilic βE190 (Fig. 5A) localized in the GER-loop (-VGER-) (Fig. 4)[7),19),54)] was also predicted by TF_1 mutagenesis producing thermophilic βE190Q.[67)] These mutant TF_1 subunits produced an $\alpha_3\beta_3\gamma$ complex that was suitable for

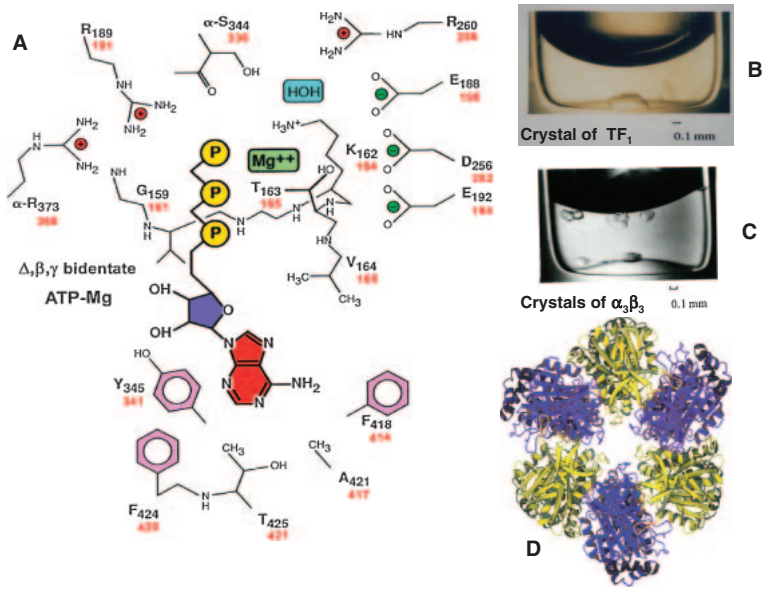

Fig. 5. Crystals of TF_1 and $\alpha_3\beta_3$, and X-ray crystallography data for the catalytic center of F_1. A. Catalytic center of the β subunit of BF_1 (black text indicates residue number)[9] and TF_1 (red text indicates residue numbers).[12] Except for αR373 and αS344, all of the amino acid residues are present in β. Residues 159–164 are part of the P-loop surrounding the triphosphate residue of ATP. B. Crystals of TF_1.[70] C. Crystals of $\alpha_3\beta_3$.[71] D. Top view of the crystallographic structure of $\alpha_3\beta_3$.[71]

experiments on torque-driven ATP synthesis.[64] Species-specific residues (black letters in Fig. 4) may have phylogenic components, including thermophilic loops (-ARNENEV-) (Fig. 4, first line I′) that render TF_1 stable.[19] Since determining the nucleotide sequence of TF_oF_1,[7),12),19] numerous rotating ATP synthases of thermophilic F-type or V-type (vacuolar ATPase) have been sequence and characterized.[65),68]

In contrast to the single operon TF_oF_1, the gene structure of HF_oF_1 is highly complex[21),26),28]; most subunits are encoded by nuclear DNA, with signal peptides to target this protein to the mitochondrial inner membrane,[21),27),28] but subunits a and A6L of HF_o are encoded by mitochondrial DNA.[21),26] The complete sequence of the 16,569-base pair human mitochondrial DNA contains genes for 12S and 16S rRNAs, 22 tRNAs, ATPase subunits 6 (corresponding to the a subunit of HF_o) and 8 (corresponds to A6L of HF_o), and 11 other protein coding genes.[26]

5. Crystallographic analysis of F_oF_1: Detailed structure of H^+-driven and ATP-driven motors

5.1. Crystallization and analysis at Photon Factory. The most detailed structural information for amino acid residues in a protein is obtained by crystallographic analysis. In 1977, a two-dimensional crystal of TF_1 showed the pseudo-hexagonal structure of $\alpha_3\beta_3$.[69] Three-dimensional crystals of TF_1 (Fig. 5B) and $\alpha_3\beta_3$ hexamer (Fig. 5C) were obtained using dye-ligand chromatography columns.[70),71] The high resolution power of the Photon Factory synchrotron (for TF_1 $\alpha_3\beta_3$, 0.32 nm resolution at Tsukuba) revealed the detailed structure of $\alpha_3\beta_3\gamma$,[9] $\alpha_3\beta_3$ (Fig. 5D),[71] the c-ring,[14),72] the peripheral stalk,[25] central stalk[29] and the stator (Fig. 2).[73] X-ray crystallography (0.325 nm resolution) of the $\alpha_3\beta_3\gamma\varepsilon$ complex of EF_1 was also recently reported (Ducan, T.M., personal communication, 2010). The peripheral stalk consists of a continuous curved α-helix about 16 nm in length in the single b-subunit, augmented by the predominantly α-helical d and F_6 (Fig. 2, right).[25]

5.2. Crystallography of F_o. The c subunits form a ring around a central pore.[14),72] The numbers of the c subunit in the F_o ring differ depending on the species: in CF_o, it is 14,[72] while that for YF_o[14] and TF_o is 10.[15] The conserved carboxylates E61 of CF_o (corresponds to E56 of TF_o) involved in proton transport, are 1.06–1.08 nm apart in the c-ring rotor, which rotates relative to the membrane anchored a subunit. The torque-generating unit consists of the interface between the rotating c-ring and the flanking stator a subunit.[14),72] The ring rotor is driven by the sequential protonation and reprotonation of E61. Residues adjacent to the conserved E61 residues

show increased hydrophobicity and reduced hydrogen bonding.[72] Upon deprotonation, the conformation of E61 is changed to another c subunit and becomes fully exposed to the periphery of the ring.[72] Reprotonation of E61 by a conserved R in the adjacent a subunit returns the E61 to its initial conformation.[72] Genetically modified TF_oF_1s, each containing a c subunit dimer (c_2) to a dodecamer (c_{12}), were prepared by genetical cross-linking.[15] Among these, TF_oF_1s containing c_2, c_5, or c_{10} showed ATP-synthesis and other activities, but those containing c_9, c_{11} or c_{12} did not. Thus, the c-ring of functional TF_oF_1 is a decamer (c_{10}).[15] When TF_1 was removed from the modified TF_oF_1s, TF_os containing only c_2, c_5 or c_{10} worked as proton channels.[15] In fact, a 36° step size of proton-driven c_{10}-ring in F_oF_1 was confirmed.[16] The c_{10} ring in YF_o[14] and functional complementation of the YF_1-deleted yeast mutant with BF_1 genes strongly suggests the presence of the c_{10} ring in HF_oF_1.[8]

5.3. Crystallography of catalytic site of F_1. The basic ground state of F_1 without nucleotides was shown on crystallography of the thermophilic $\alpha_3\beta_3$ hexamer,[55] in which three $\alpha_1\beta_1$ dimers[55] were arranged in three-fold symmetry, 12 nm across and 10 nm high (Fig. 5D).[71] The first detailed crystallography of nucleotide-bound $\alpha_3\beta_3\gamma$ (partial) of BF_1 was determined at 0.28-nm resolution by Walker's group.[9] In the structure of BF_1 crystallized in the presence of ligand (AMPPNP:ADP:Pi = 50:1:0, and Mg^{2+}), the three catalytic β subunits differed in conformation and in bound nucleotide. There were four unhydrolyzable ATP analogue (AMPPNP) molecules, three in equal three α subunits, one in β (β_T) and one ADP in β (β_D); the remaining β was empty (β_E).[9]

The ATP-binding site of β_T is surrounded by the residues shown in Fig. 5A (black numbers for BF_1 are identical to those of HF_1, red numbers for TF_1).[9),71] In the P-loop of β_T of TF_1, the essential K164[20] forms hydrogen bonds with the phosphate of the nucleotide, and the oxygen of T165 coordinates with Mg^{2+}, while in the GER-loop, E190 interacts with water (Fig. 5A).[9),71] The catalytic activity of β requires α that supplies thermophilic α-R365 and thermophilic α-S336 to the ATP-binding site at the $\alpha\beta$ interface (Fig. 5A).[9),71),74] The positive charge of α-R365 stabilizes the β-phosphate of AT(D)P, and R256, R191 and K164 of thermophilic β interact with the negative charges of the phosphates of AT(D)P (Fig. 5A). The cross-linking of thermophilic βY341 with azido-ATP[7),54] predicted a hydrophobic interaction between the adenine ring, and Y341, F414 and F420 (Fig. 5A).[9),71]

5.4. Basic structure of $\alpha_3\beta_3$ is rendered asymmetric by addition of γ and/or nucleotides. The basic structure of F_1 is a symmetrical $\alpha_3\beta_3$ hexamer that is composed of three pairs of alternating α_E and β_E (Fig. 5D).[71] However, the asymmetry induced by introduction of γ and/or AT(D)P to $\alpha_3\beta_3$ hexamer is critical in the mechanism of ATP synthesis.[9] The nucleotide-free β_E in both the F_1 crystal[9] and solution[56] has an open structure (Fig. 6) that is essentially identical to β_E in the nucleotide-free $\alpha_3\beta_3$ hexamer.[71] Both β_T and β_D, as well as α_T, assume closed structures (Fig. 6, direction of the open arrow).[9] Interconversion of the open-close conformational states of β is achieved by addition of AT(D)P to the isolated β_E of TF_1.[6),56] However, nucleotide-free YF_1 contained β_D and β_T structures similar to those of nucleotide-bound BF_1.[75] This suggests that $\beta\gamma$ interactions at the three contact points (Fig. 6, middle, γ1–3), including interaction of Arg residue at position 75 (γR75) with β_DE395 in the DELSEED sequence of BF_1 to change the mutual conformation,[10),14] are as important as nucleotide occupancy in converting open β_E into the closed β.[75] As genes for α, β and γ of YF_1 in the α-β-γ deleted mutant yeast are complemented with those of BF_1,[8] the functional residues are essentially equal between YF_1 and $B(H)F_1$. Occupancy of the catalytic site by ATP or ADP can be mimicked by convenient BeF_3-ADP complexes that bind to the catalytic sites of β_T and β_D.[76] The structure is representative of an intermediate in the reaction pathways.[76] The conformational change of β induced by γ-rotation is essential for ATP synthesis (ATP release from the catalytic site), while that induced by ATP-binding to β is necessary to elicit torque on γ.[74),75]

5.5. Three domains in α and β: β barrel, nucleotide-binding and α-helical bundle domains. The overall molecular structure of α and β can be divided into three domains[9),71),75]: an N-terminal β barrel (Fig. 6, top N to *), a central nucleotide-binding domain (Fig. 6, middle * to **), and a C-terminal α-helical bundle (Fig. 6 bottom ** to C).[7] The locations of amino acid residues in the α-helices (Fig. 4, solid black lines A–H, 1–8) and β-sheets (Fig. 4, solid black lines a–f, 0–8)[71),74] are compared in the three-dimensional structure of thermophilic β (Fig. 6). As the amino acid sequence of BF_1[24] is nearly identical to that of HF_1 (99% homology in β),[19),21] the following discussion on BF_1

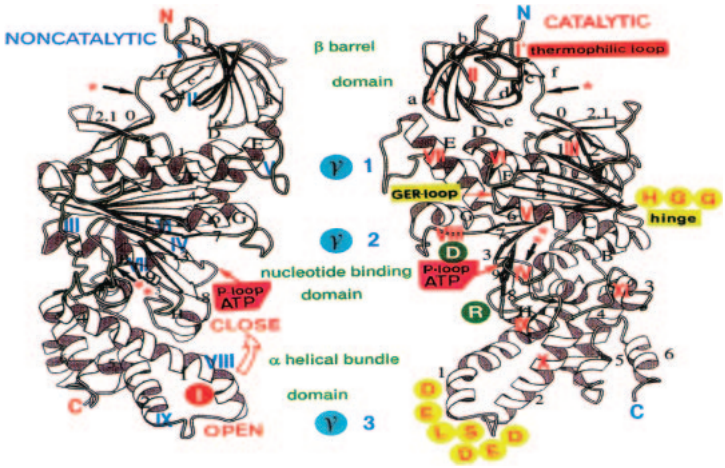

Fig. 6. Three-dimensional structures of Tβ_E. Three-fold axis is vertical, so that views are towards the $\alpha\beta$ subunit interfaces. Left: non-catalytic interface (blue I–IX indicates contact areas). Right: catalytic interface (red I–XI indicates contact areas). Green letters: domain names, with domain borders being marked by red asterisks. D and R in green circles are TβD331 and TβR333, respectively, at the entrance to the crevice of the P-loop. I in red circle is TβI386 of $\beta\beta$ contact. H and G in yellow circles indicate hinge residues in Tβ (179–181).[74]

is also applicable to HF_1. Superposition of the overall crystallographic structures of thermophilic β_E and bovine β_E or bovine α revealed that the folding of these structures is very similar.[9),71)] The β barrel domains (Fig. 4, Tα 21–94, Tβ1–82) contain six β strands (Fig. 6. plate form arrows, βa–βf).[74)] The nucleotide-binding domains (T α95–371, Tβ83–354) consist of nine-stranded β-sheets surrounded by eight α-helices (Fig. 6, αA to αH) and a small antiparallel β-sheet. The C-terminal α-helical bundle domain of α (thermophilic α375–502) contains six helices (Fig. 4, α1, 2, 4, 6–8), while that of β (theromophilic β355–473) consists of six α-helices (Fig. 4, α1–6). Thus, the largest difference between α and β is found in the C-terminal region,[9),74)] and the DELSD(E)ED sequence localized in this region was shown to be the most important $\beta\gamma$ contact area.[10)]

5.6. Catalytic and non-catalytic $\alpha\beta$ interfaces and conformational change. The crystal structure of BF_1[9)] and $\alpha_3\beta_3$ of TF_1[71)] indicates that, in general, the conserved residues lie on the $\alpha\beta$ interfaces, as shown by detailed homology search among TF_1, HF_1, CF_1 and EF_1.[19)] There are two types of $\alpha\beta$ interface that contain either a catalytic site or non-catalytic site.[9),74),75)] The area where pairs of residues connecting the $\alpha\beta$ interface are located is defined as contact area. Contact residue pairs within a limit of 0.40 nm across the $\alpha\beta$ interfaces in BF_1 and the $\alpha_3\beta_3$ hexamer of TF_1 were analyzed by a computerized atom search using the CCP4 Suite: Program Contact.[74)] The contact areas composed of homologous residue pairs found in both TF_1 and BF_1 were defined as homological contact areas. The contact areas found only in one species, such as the thermophilic loop of TF_1 (I′ in Fig. 4) were defined as species specific contact areas. These areas are expressed as primary structure in Fig. 4. The contact areas are located in both β and α at catalytic (red and pink bars in Fig. 4), and non-catalytic (blue and green bars in Fig. 4) interfaces. There are seven catalytic (red I–III, V–VIII in Figs. 4 and 6) and non-catalytic (blue I–VII in Figs. 4 and 6) contact areas on the open β form (β_E). The number of contact areas on closed β (β_D and β_T) increased to 11 (red I–XI in Fig. 6) and 9 (blue I–IX in Fig. 6), respectively, in the catalytic and non-catalytic interfaces. The barrel domain harbors the universal contact areas I and II (Fig. 6, upper), and the common electrostatic bond in II is thermophilic βR72–thermophilic αE67 (=human βR71–human αE67).[9),71)] At the catalytic nucleotide-binding domain, areas III, V, VI, VII and VIII are universally detected (Fig. 4). However, in Tβ_E, the P-loop contact area IV is latent, in contrast to that area in thermophilic αE (Fig. 6). Human αR373 interacts with oxygen in the β- and γ-P of ATP bound at IV.[9)] In V, the common electrostatic bonds are thermophilic βR193–αD339. In VI and VII of β_T and β_D, human αF299–βM222 and human αS344–βR260, respectively, interact. However, we identified no direct contact in the α-helical bundle domain in β_E of TF_1.[74)] In the catalytic $\alpha\beta$ interface of human β_E, the contact areas (17.6 nm^2) are

homologous to those of thermophilic β, while the areas in human β_D (30.3 nm^2) and human β_T (22.0 nm^2) are increased to 11 and 10, respectively. This is caused by the 30° upward motion of the C-terminal domains.

5.7. Catalytic sites. The catalytic $\alpha\beta$ interface is located on the left side of β in the $\alpha_3\beta_3$ hexamer (Fig. 5D), and the structure of catalytic domain (Fig. 5A) is strictly conserved among species.[7),9),71),74)] The catalytic domain accommodates the P-loop located between sheet 3 and helix B (Tβ163–178) and the conserved thermophilic βE190 (=human βE188) in the GER loop localized between β-sheet 4 and N-terminal end of α-helix C[9)] (Fig. 4, GER, and Fig. 6, middle). As predicted by X-ray crystallography of AMPPNP-BF_1,[9)] NMR analysis revealed that thermophilic βR191 (Fig. 5A, upper left) forms a hydrogen bond with the γ-phosphate of ATP.[56)] Pi is shown to bind the catalytic domain of β_E,[62),75)] which is identical to the sulfate binding site of β_E in $\alpha_3\beta_3$ by βK164 and αR365.[71)] The structure of the active metal-ATP complex in TF_1 at the catalytic domain was shown to be Δ, β, γ-bidentate Mg-ATP.[77)] (Rp)-[$\beta\gamma$-^{18}O, γ-^{18}O]ATPγS was hydrolyzed by TF_1 in $H_2{}^{17}O$, and the resulting inorganic [^{16}O, ^{17}O, ^{18}O] thiophosphate was shown to have an Rp configuration.[77)] The reaction thus proceeds with inversion of configuration at the phosphorous, and a direct in-line nucleophilic attack of the ^{17}O in water on the γ-phosphate of ATP *via* the pentavalent intermediate state.[77)] The ordered water molecules that carry out nucleophilic attack on the γ-phosphate of ATP during hydrolysis are 0.26 nm from the nucleotide analogue, beryllium, in the β_D and 0.38 nm away in β_T, strongly indicating that β_D is the catalytically active conformation.[76)]

Adjacent to the P-loop, there is a hinge point, -HGG (179–181), between α-helix B and β-sheet 4 (Figs. 4, hinge, and Fig. 6, right). The conformational change in the hinge should be transmitted to the DELSDED sequence in α-helix I. The hinge motion of the C-terminal domain containing the DELSDED sequence in thermophilic β_E, rotated away from the core axis from 110° (close) to 144° (open)[56)] In the reverse reaction, the resulting widening of the P-loop–thermophilic βE190 distance causes the release of Mg-ATP from the catalytic site.

Crystallographic analysis of the F_1–IF_1 complex (IF_1: natural inhibitory peptide) at 0.28-nm resolution revealed that IF_1 binds in the α_D–β_D interface and opens the catalytic site.[78)] Inhibitor studies on F_1 are thus important in understanding the formation of dimeric HF_oF_1 and prevention of futile ATP loss when $\Delta\mu H^+$ is decreased, as described in section 10.

6. Nanotechnological analysis of TF_oF_1 by single-molecule imaging: Dynamic movement of F_oF_1

X-ray crystallography of F_1 and F_oF_1 is a static snapshot of inhibited ATPase crystallized in the presence of AMPPNP[9)] or BeF_3,[76)] or in the absence of nucleotides.[71),75)] These crystals do not represent the transient movement of subunits of TF_1 during γ-rotation, or activity of TF_oF_1 in a liposome.[3),39),46)] Thus, the dynamics of rotating TF_1[79)] or ATP synthesis in F_oF_1-liposomes[80)] must be measured by using TF_1 containing mutant β subunits,[63)] and also using modalities such as fluorometry[79),80)] or NMR.[56)]

The efficiency of florescence resonance energy transfer (FRET) between a donor and an acceptor fluorophore depends on their distance.[16),79),80)] If two fluorophores are bound to appropriate amino acid residues in rotor and stator subunits, relative subunit movements can be observed in real time by confocal microscopy.[16),79),80)]

6.1. Nanomotor movement analysis by single-molecule FRET. In a single TF_1 molecule fixed on a glass surface,[11),63)] a donor fluorophore (Cy3) was bound to one of the three βs and an acceptor fluorophore (Cy5) was bound to the protruding portion of γ, and single pair (Cys3–Cys5) FRET was performed to estimate the waiting conformation during ATP hydrolysis.[79)] As Cy3- and Cy5-maleimide are bound to cysteine residues, site-directed mutagenesis [α(C193S), β(S205C) and γ(S107C)] was performed to bind Cy5 to β, and to bind Cy3 to γ, and to prevent binding of Cy3 and Cy5 to α (residue numbers of α and β are indicated in Fig. 4).[79)] The sole cysteine in a mutant subcomplex of TF_1, α(C193S)3β(His-10 tag at N terminus) 3γ (S107C), was labeled with Cy5-maleimide. The (Cy5-γ)TF_1 was incubated with Cy3-β(S205C) at 1:10 at 45°C for 2 days, and the free β subunit was removed on a size exclusion column.[79)] The energy of the laser beam (532 nm) on Cy3 was transferred to Cy5 and emitted light (670 nm) when the Cy3–Cy5 distance was small, while only Cy3 light (570 nm) was emitted when the Cy3–Cy5 distance was great. FRET yield changed cyclically as γ rotated and the Cy3–Cy5 distances were estimated during the conformation change.[79)] The distance between the two dyes changed continuously as 5.7, 7.9, and 7.9 nm during rotation at low ATP concentrations, and the conformational change corresponded to the ATP-waiting state of TF_1.[79)]

The relative subunit movement during ATP synthesis has also been measured by FRET between two fluorophores bound to a stator subunit (b-subunit) and a rotor subunit (γ- or ε- or c-subunit) (Fig. 1).[62),80)] The labeled F_oF_1 was reconstituted in the liposome (one F_oF_1 per liposome) and $\Delta\mu H^+$ was applied, so that F_oF_1 carried out H^+-driven ATP synthesis.[46)] Analysis of the time course of FRET efficiency in the F_oF_1-liposome showed the rotation of γ- and ε-subunit relative to b-subunit in 120° steps,[80)] and that of the c_{10}-ring in 36° steps.[16)] The β motions through an attached fluorophore, concomitantly with the 80° and 40° substep rotations of γ in the same single molecules, showed the sequence of conformations that each β undergoes in three-step bending, an approximately 40° counterclockwise turn followed by two approximately 20° clockwise turns, occurring in synchronization with two substep rotations of γ.[80)] The results indicate that most previous crystal structures mimic the conformational set of three βs in the catalytic dwells,[80)] while the previously described set of β_E, β_D and β_T was revealed in the ATP-waiting dwells.[80)] These fluorescent studies thus bridge the gap between the chemical and mechanical steps in F_oF_1. Starting from the ATP-waiting dwell (0°), the 80° and 40° substeps of γ rotation are induced by ATP binding and ADP release, and ATP hydrolysis and Pi release, respectively.[62),79)–81)]

6.2. H^+/ATP ratio and elastic power transmission in F_oF_1. One of the unsolved questions in the mechanistic study is the analog–digital conversion of energy in F_oF_1. The electrochemical energy of the H^+ current[1)] through F_oF_1 in liposomes[3)] and planar bilayers,[51)] and the electric,[48),50)] magnetic[64)] and mechanical energy of the rotation[11),62)] are all analog quantities. The numbers of ATP molecules synthesized and protons transported are digital quantities. Thus, the elastic power transmission in F_oF_1 analog/digital conversion during the γ-rotation was predicted in 1996.[10)] Oosawa also proposed a loose coupling mechanism in which the number of protons necessary for the synthesis of one ATP is not an integer but varies depending on the environmental conditions.[61)] As one proton is translocated by one shift of c_{10} in the c-ring of TF_oF_1,[15),16)] and one ATP is synthesized per β subunit of TF_1, the inevitable consequence is noninteger ratios of rotation step sizes for TF_oF_1 (120°/36°) and for H^+/ATP (10:3).[14),15),74)] This step-mismatch necessitates elastic twisting of TF_oF_1 during rotation and elementary events in catalysis.[7),74)] The H^+/ATP ratio in F_oF_1 addresses this analog/digital problem. F_os with c_{10} ring are present in organisms that maintain $\Delta\mu H^+$ mainly in the form of $\Delta\psi$,[14),15)] whereas F_os with c_{14} ring are mostly found in species with $\Delta\mu H^+$ existing predominantly in the form of ΔpH rather than $\Delta\psi$.[72)] H^+/ATP ratios of 4.7 and 3.3 are thus expected for CF_oF_1 (with $14c/3\beta$)[72)] and $E(T)F_oF_1$ (with $10c/3\beta$),[14)–16)] respectively. To confirm the effects of c/β subunit ratios on H^+/ATP ratio, pH of the internal phase of the reconstituted F_oF_1-liposomes was equilibrated with acidic medium.[46),47)] Then, an acid-base transition[46)] was induced by adding alkaline medium to the liposomes to produce ΔpH across the membrane, and the initial rate of ATP synthesis was measured with luciferase.[82)] From the shift in the equilibrium ΔpH as a function of Q ($= [ATP]/([ADP][P_i])$, the standard Gibbs free energy for phosphorylation, $\Delta G_p^{0'}$, and the H^+/ATP ratio were determined.[82)] The results were as follows: $\Delta G_p^{0'} = 38 \pm 3$ kJ/mol and $H^+/ATP = 4.0 \pm 0.2$ for CF_oF_1; and $H^+/ATP = 4.0 \pm 0.3$ for EF_oF_1. This indicates that the thermodynamic H^+/ATP ratio is the same and that it differs from the subunit c/β stoichiometric ratio.[82)] However, in order to estimate actual energetics, the very low turnover rates (<1 ATP/s) in this experiment[82)] need to be examined under different physiological conditions (>100 ATP/s).

The site of analog–digital conversion by elasticity[7)] was estimated by direct measurement of the torsional stiffness.[83)] Most parts of F_1, particularly the central γ shaft in F_1, and the long eccentric bearing had high stiffness (torsional stiffness $\kappa >$ 750 pN nm).[83)] One domain of the rotor, namely, where the globular portions of γ and ε contact the c-ring, was more compliant (κ congruent with 68 pN nm).[83)] The γ-induced or nucleotide-dependent open–close conversion of conformation is an inherent property of an isolated β, and energy and signals are transferred through $\alpha\beta$ interfaces.[7),11),74)] Rotation of the central shaft γ in $\alpha_3\beta_3$ hexamer is assumed to be driven by domain motions of the βs. These β motions were directly observed through an attached fluorophore by FRET[79),80)] and NMR.[56)]

The mechanisms underlying the open(β_E)–close(β_T) motion were investigated for β subunit of TF_1 in solution, using mutagenesis and NMR.[56)] The hydrogen bond networks involving side chains of K164 (162 for human β is shown in parentheses), T165(163), R191(189), D252(256), D311(315) and R333(337) in the catalytic region (Fig. 5A, red text for TF_1 and black text for HF_1)[74)] are significantly different for the ligand-bound and free β subunits.[56)] The role of each amino acid residue was examined by

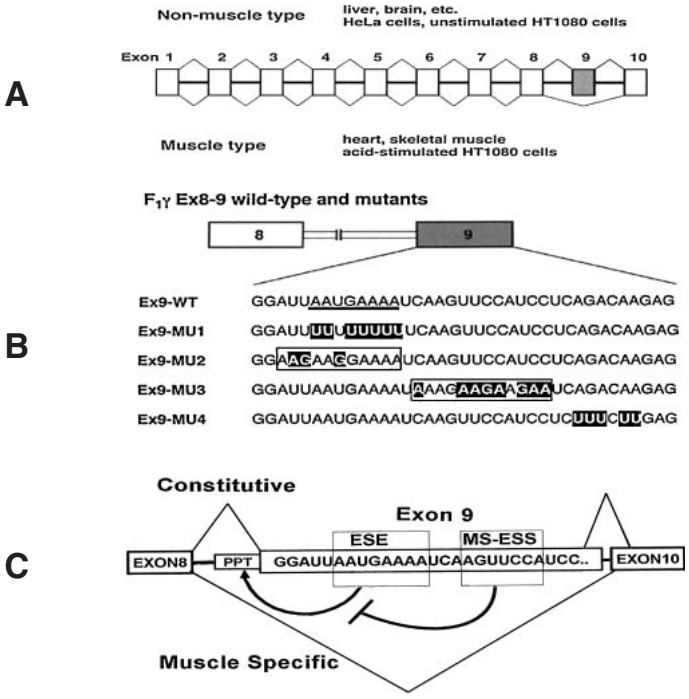

Fig. 7. Alternate splicing of human $F_1\gamma$ pre-mRNA. A. Exons in the F_1 γ pre-mRNA are expressed in boxes. Exon number 8 (hatched box) is included in liver and excluded in the muscle. B. Schematic representation of wild-type and mutant $F_1\gamma$ exons 8–9 (Ex8–9).[27] Heavy underline in Ex9-wild-type indicates ESE element. Mutated nucleotides are indicated by outlined letters. In Ex9-MU2 and Ex9-MU, boxed letters indicate that these sequences are predicted to act as ESE elements. C. Selection of $F_1\gamma$ exon 9 is regulated by two cis-acting regulatory elements in the same exon.[90] Purine-rich ESE promotes exon 9 inclusion, which is repressed by MS-ESS under muscle-specific conditions; PPT: Polypyrimidine tract.

A (alanine) substitution.[56] The chemical shift perturbation of backbone amide signals of the segmentally labeled β(mutant)s indicated stepwise propagation of the open/close conversion on ligand binding.[56] Upon ATP binding, the open/close conformation change regulated by hydrogen-bond switching from K164/D252 to T165/D252 (Fig. 5A, right upper, red test) would take place in the thermophilic β subunit because ATP-binding is the major driving force for the first 80° rotation.[62] The resulting closing motion of the hinge (-HGG-) between α-helix B and β-sheet 4 (Fig. 6, right) generates the torque of γ rotation through the DELSD(E)ED contact point (Fig. 6, bottom).[10),56] Although the time scale of atomic fluctuations is in the order of tens of nanoseconds, molecular simulation will solve the detailed movements of residues in $\alpha_3\beta_3$ during the γ rotation (order of milliseconds) in the future.

7. Biogenesis of human F_oF_1: Regulated expression, splicing, import and assembly

The biogenesis of HF_oF_1 is an intricate process,[21] starting from transcription,[84)–86] splicing of nuclear encoded subunits (Fig. 7),[27),32] and translation of mitochondrial DNA-encoded subunits (Fig. 8)[22),26),87] and nuclear DNA-encoded precursor peptides for all F_1 subunits (α, β, γ, δ and ε)[21),86] and 7 F_o subunits (b, c, d, e, f, g and OSCP),[21] followed by targeting, importing and processing of nuclear DNA-encoded precursor peptides in the mitochondrion (Fig. 9).[21),86] Precursor importing requires both $\Delta\mu H^+$ to drive translocation and specific carrier proteins in the outer and inner mitochondrial membrane, as well as general chaperones present in the cytosol and mitochondrial matrix.[86] Processing of the presequence of precursor requires a specific protease,[86] and after the removal of the presequence, nuclear-encoded subunits are assembled into HF_oF_1 with two mtDNA-encoded F_o subunits (a and A6L).[87] Targeting the presequence of three isoforms of subunit c liberated after proteolysis is required for the assembly of cytochrome oxidase.[88]

As both the amino acid and nucleotide sequences of subunits in HF_oF_1 are available in internet databases, only physiologically important points

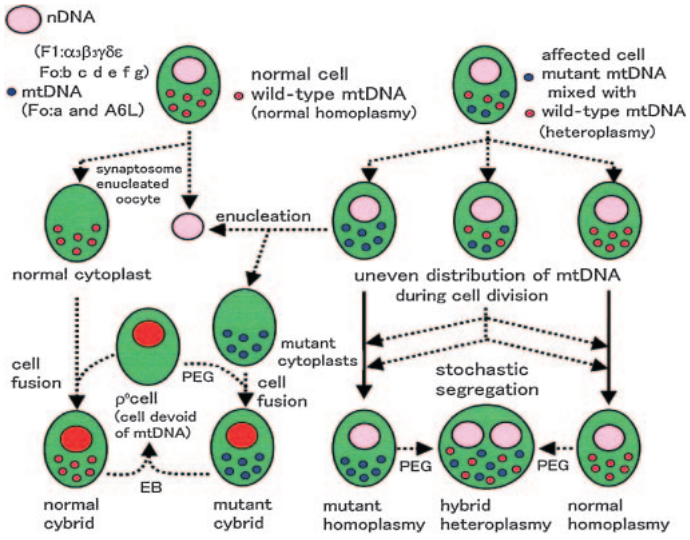

Fig. 8. Homoplasmy, heteroplasmy, cytoplasts and ρ^o cells.[87] Small red circles indicate wild-type mtDNA and small blue circles indicate mutant mtDNA; large red circles indicate nDNA, and green ovals indicate cells. EB: ethidium bromide used to remove mtDNA; PEG: polyethylene glycol used to fuse cells or cytoplasts.

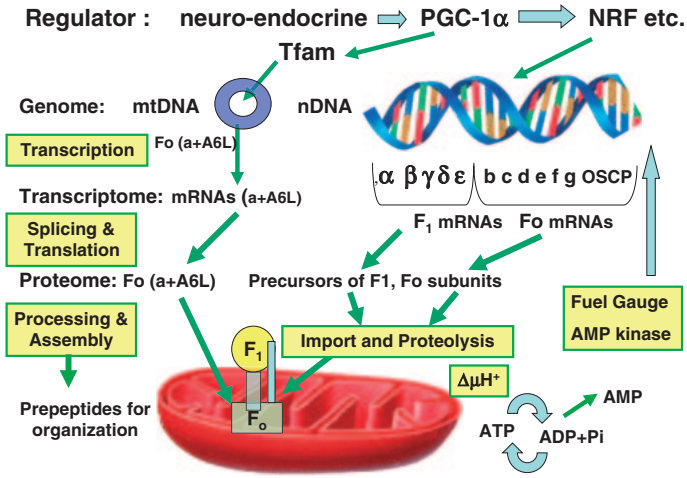

Fig. 9. Regulation of HF_1F_o biosynthesis[21),86)]: Transcription, splicing, translation, targeting, import, processing and assembly. PGC-1α: Peroxisome proliferator-activated receptor-γ coactivator-1α; Tfam: mitochondrial transcription factor A; NRF: nuclear respiratory factor; Circle: mitochondrial DNA.

in the biogenesis of HF_oF_1 will be reviewed here.[21),28),86),89)] In contrast to prokaryotic F_oF_1, including TF_oF_1,[7)] proteomics have revealed a large universe of pseudogene products,[21),84)] splice variants (muscle-type $F_1\gamma$) (Fig. 7),[27),32),90)] post-translational modifications (phosphorylated HF_oF_1, *etc.*),[91)] dimeric HF_oF_1,[30)] a supramolecular complex called ATP synthasome (Fig. 2),[31)] and ectopic HF_oF_1 (Fig. 10, right).[92)]

7.1. Expression of HF_oF_1 genes. The gene structure of the $HF_1\alpha$ subunit is 14 kbp in length and contains 12 exons interrupted by 11 introns.[21),84)] Primer extension and S1 mapping analysis showed the presence of multiple transcription initiation sites in the $HF_1\alpha$ gene.[84)] The 5′-flanking region of the $HF_1\alpha$ gene has an unconserved GC-rich region, including several binding motifs of transcriptional factors, such as Sp1, AP-2 and GCF. The basal promoter activity was located near the GC-rich region. Comparison of the 5′-upstream region of the $HF_1\alpha$ gene with those of the genes for $BF_1\alpha$, $HF_1\beta$[85)] and $HF_1\gamma$[27)] indicated three common sequences (CS1,

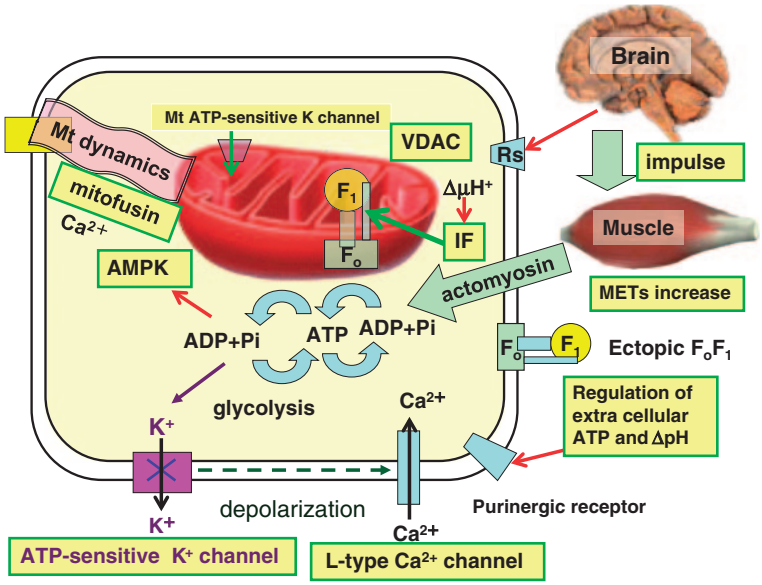

Fig. 10. Regulation of HF_1F_o activity: Neuronal impulse from brain to human activity driven by ATP by an intricate regulation system. AMPK, AMP kinase; ecto-F_1F_o, ectopic or cell surface F_1F_o; IF, ATPase inhibitor; METs, metabolic equivalents of exercise intensity; Rs, receptors for neuro-endocrine transmitters; VDAC, voltage-dependent anion channel.

CS2 and CS3) in the regulatory regions,[21] suggesting that putative *cis*-elements coordinate the expression of the three subunit genes for HF_1.[84)–86)] The enhancer activities derived from 5′-deletion mutants of a $HF_1\alpha$-CAT (chloramphenicol acetyltransferase) chimeric gene were different in cell lines from four different human tissues, thus suggesting the existence of cell type-specific gene regulation.[21]

The $HF_1\beta$ gene is 14 kbp in length and contains 10 exons, with the first exon corresponding to the non-coding region and most of the presequence, which targets this protein to the mitochondria.[85),86)] Eight Alu repeating sequences including inverted repeats were found in the 5′-upstream region and introns. An S1 nuclease protection experiment revealed two initiation sites for transcription. Three CCAAT boxes were found between the two initiation sites, and two GC boxes were located in the 5′-upstream region. Promoter activity was estimated by the CAT method and an enhancing structure for transcription was detected between nucleotides -400 and -1100 in the upstream region.[86]

The system coordinating expression of nuclear-coded mitochondrial proteins was investigated by examining the 5′-flanking region of the $HF_1\beta$ gene. In one of the enhancing regions, a consensus sequence was found for the genes of other mitochondrial proteins, such as those for cytochrome c_1 and the pyruvate dehydrogenase α-subunit.[21),86)] The characteristics of this enhancing element were examined by introducing a synthetic oligonucleotide element into the CAT plasmid with a deleted enhancing element. The resulting plasmid showed full recovery of promoter activity, and this activity was independent of the orientation or location of the insert. Therefore, this enhancer may be common to the nuclear genes of some mitochondrial proteins involved in energy transduction.[21]

The functions of subunits in mitochondrial F_oF_1 were confirmed by expression of genes in deletion mutants, and their functional complementation.[8] The genes encoding BF_1 subunits (except for those of δ) were expressed in a quintuple yeast YF_1 deletion mutant ($\Delta\alpha\Delta\beta\Delta\gamma\Delta\delta\Delta\varepsilon$) after introduction of a chimeric BF_1 subunit gene construct that uses the YF_1 transcriptional promoter and termination sites, as well as the presequence for YF_1.[8] Expression of the α-, β-, γ-, or ε-subunit of BF_1 complemented the corresponding individual mutations in YF_1. All BF_1 subunits (with chimeric δ) expressed in yeast produced an F_1 that was purified to a specific activity of about half of that of original BF_1.[8] These results indicate that the molecular machinery required for the targeting, proteolysis and assembly of the mitochondrial F_oF_1 is conserved from yeast to humans (Fig. 9).[8] Similarly, bovine OSCP and some

F_o components have been functionally complemented (quoted in Ref. 8). In one functional study, the gene for γ subunit (atp-3) was partially blocked by RNA interference (RNAi) in *Caenorhabditis elegans*, and ATP levels decreased from 15 nmol/mg protein (control) down to 4 nmol/mg, and the behavior extended the lifespan.[93] However, tissue differentiation is absent in yeast, alternate splicing must be studied in human cells.[27),32]

7.2. Tissue-specific splicing of $HF_1\gamma$: Analysis using transgenic mice and minigenes. Mammalian F_oF_1 is characterized by tissue-specific expression of the F_1 gene, which was analyzed using transgenic mice[32] and minigenes in cultured human cells.[90] The muscle-specific isoform of $HF_1\gamma$ was generated by alternative splicing, and exon 9 was found to be lacking in skeletal muscle and heart tissue (Fig. 7, A).[27] Using transgenic mice,[32),90] the alternative splicing of exon 9 was shown to require *de novo* protein synthesis of a *cis*-acting element on the spliced exon of $HF_1\gamma$ gene. An $HF_1\gamma$ wild-type minigene, containing the full-length gene from exons 8 to 10, and two mutants were prepared; one mutant involved a pyrimidine-rich substitution on exon 9, whereas the other was a purine-rich substitution (abbreviated as $HF_1\gamma$ Pu-del and $HF_1\gamma$ Pu-rich mutants, respectively).[90] Pu-del inhibited exon inclusion, indicating that a Pu-del mutation disrupts an exonic splicing enhancer. On the other hand, Pu-rich blocked muscle-specific exon exclusion.[90]

Transgenic mice bearing both mutant minigenes were then analyzed for their splicing patterns in tissues.[90] Based on an analysis of $HF_1\gamma$ Pu-del minigene transgenic mice, the purine nucleotide in this element was shown to be necessary for exon inclusion in non-muscle tissue. In contrast, analysis of $HF_1\gamma$ Pu-rich minigene mice revealed that the $HF_1\gamma$ Pu-rich mutant exon had been excluded from heart and skeletal muscles in these transgenic mice, despite the fact that mutation of the exon inhibited muscle-specific exon exclusion in myotubes at early embryonic stages.[32] These results suggest that the splicing regulatory mechanism underlying $HF_1\gamma$ pre-mRNA differs between myotubes and myofibers during myogenesis and cardiogenesis.[32]

A detailed mutational analysis of exon 9 (Fig. 7, B) revealed a purine-rich exonic splicing enhancer (ESE) element (5′-AAUGAAAA-3′) functioning ubiquitously, with the exception of muscle tissue. An exonic negative regulatory element responsible for muscle-specific exclusion of exon 9 was discovered using both *in vitro* and *in vivo* splicing systems.[32),90] Mutation analyses on the $HF_1\gamma$ Ex8-9 minigene using a supplementation assay demonstrated that the muscle-specific negative regulatory element is positioned in the middle region of exon 9, immediately downstream from ESE. Detailed mutation analyses identified a muscle-specific exonic splicing silencer (MS-ESS) (5′-AGUUCCA-3′) responsible for exclusion of exon 9 *in vivo* and *in vitro* (Fig. 7, C).[90] This element was shown to cause exon 9 skipping of *in vivo* splicing systems.[90] Although there are three variants of the c subunit[88] and several alternate splice variants in the human mitochondrial fusogenic proteins (mitofusin 1, 2),[87] the γ subunit of HF_1 is the only well-characterized variant in F_oF_1.[86),90]

8. Mitochondrial cytology of HF_oF_1: cytoplasts lack nDNA and ρ^o cells lack mtDNA

HF_oF_1 is encoded by both mitochondrial DNA (mtDNA)[22),26),33] and nuclear DNA (nDNA) (Fig. 9).[21),86] In order to analyze the roles played by mtDNA and nDNA, mtDNA-less cells (ρ^o cells)[22),33] and nDNA-less cells (cytoplasts) were developed (Fig. 8).[87),94] Using ethidium bromide, mtDNA was removed and the resulting ρ^o cells became strictly dependent on glycolysis to compensate for the oxphos that supplies ATP.[33),87] Thus, a glucose medium is essential for ρ^o cells.[22] Cytoplasts are enucleated cells that contain mitochondria (Fig. 8, upper left), with examples being enucleated oocytes,[87] synaptosomes[94] and platelets.[94] Since DNA sequence of an individual differs from each other owing to the genetic polymorphism of mtDNA,[21] personal collection of mtDNA is essential to elucidate mitochondrial diseases. Human mitochondria with intact mtDNA have been directly isolated from postmortem platelets.[94] Expression of nDNA-encoded HF_oF_1 subunits was not affected in ρ^o cells,[87] while that of mtDNA-encoded HF_o subunits (F_oa and A6L) was lost in cytoplasts, as nDNA-encoded mitochondrial transcription factor A (Tfam)[95] was lacking (Fig. 9).[87] The ρ^0 cells have no respiratory chain, because of the loss of mtDNA-encoded subunits of cytochromes and NADH dehydrogenase.[26),87] Despite the absence of oxphos, ρ^o cells require mitochondrial compartments with a sufficient $\Delta\mu H^+$ for energy driven transport of matrix components.[87),96] The essential $\Delta\mu H^+$ of ρ^o cells is maintained by the electrogenic exchange of ATP^{4-} for ADP^{3-} by ANC.[96] To energize the inner membrane, $\alpha_3\beta_3$ (ATPase active)[55] in the matrix of ρ^o cells regenerates ADP from translocated ATP.[96]

The term heteroplasmy refers to cells that contain a mixture of mtDNAs with different sequences (Fig. 8, upper right), whereas homoplasmy means that 100% of their mtDNA has an identical sequence (Fig. 8, upper left).[22),87)] Cybrids were formed by cytoplast fusion with ρ^o cells using polyethylene glycol (PEG) (Fig. 8, bottom).[87),94)] The majority of pathogenic mtDNA mutations are heteroplasmic, with mutated and wild-type mtDNA coexisting in the same cell (Fig. 8, upper right).[86),87)] Owing to the absence of protecting histones, mtDNA is highly susceptible to mutations that result in heteroplasmy. Mutations in the tRNA gene of mtDNA often block translation and cause complete deletion of mtDNA-encoded proteins (*syn*$^-$ mutation), including HF_o subunits.[87)]

During development, cell division unevenly distributes heteroplasmic mtDNA into daughter cells and eventually segregates homoplasmic cells with wild-type and *syn*$^-$ mutant mtDNA (Fig. 8, bottom right). This stochastic segregation of the *syn*$^-$ mutation results in the *syn*$^-$ mutant concentrated tissues and causes mitochondrial diseases, including mitochondrial diabetes.[87)] The homoplasmic *syn*$^-$ cells lack oxphos and depend on glycolysis. Under the influence of polymorphisms in mtDNA and nDNA, a vicious circle of reactive oxygen species will damage cells. However, mitochondrial transfer from wild-type homoplasmic cytoplasts by fusion to form cybrids will normalize the diseased cells[97)] and *syn*$^-$ mutation will be alleviated by mitochondrial fusion.[87),97)] We analyzed heteroplasmy and polymorphisms related to diabetes and its complementation by mitofusins.[87)] Mitochondria in human cells are visualized as a network or as filaments that undergo continuous changes in shape and in localization within the cells. Mitochondrial fusion proteins including mitofusins[87)] and OPA1[98)] that may work as natural PEG in Fig. 8,[87)] and regulate both mitochondrial fusion and metabolism. We characterized splice variants of human mitofusins (also called hfzo 1, 2 and 3)[87)] as well as OPA1s (Fig. 10, upper right).[98)] We analyzed complementation by fusogenic proteins, and the lost tRNA in mitochondria of *syn*$^-$ mtDNA inside heteroplasmic cells was complemented by wild-type tRNA in normal mitochondria by fusing wild-type and *syn*$^-$ mitochondria with mitofusins.[87)] The mitofusin genes were expressed mainly in post-mitotic brain and muscle, thus complementing mutated mtDNA that is not removed during cell division.[87)]

In order to analyze a mitochondrial disease, pure nuclear transfer was carried out from ρ^0 HeLa cells to the fibroblast lines from a patient with cardiomyopathy, and their nuclear hybrid clones were isolated.[22)] A normal fibroblast line from the fetus and a respiration-deficient fibroblast line from the patient were used as positive and negative controls, respectively.[22)] By this method, many mitochondrial diseases devoid of HF_o have been elucidated[87)] and mitochondrial gene therapy for heteroplasmic patients was developed using cytoplasts from a normal fetal cells and the cybrids (Fig. 8).[97)]

The most frequent mutation in mtDNA-encoded HF_o gene is NARP (neuropathy, ataxia, and retinitis pigmentosa), caused by a mutation at L156 in the a subunit of HF_o (Fig. 2).[99)] A mutation conferring a milder phenotype (L156P) leads to a 30% reduction in H^+ flux, and a similar loss in ATP synthesis. The more severe mutation (L156R) also leads to a 30% reduction in H^+ flux, but ATP synthesis is abolished.[99)] With the L156P mutation, rotation of the c-ring may be slowed, but coupling of ATP synthesis to H^+ flux is maintained (Fig. 1, lower left, subunit a), whereas with the L156R mutation, H^+ flux is uncoupled, because the transmembrane helix III of F_oa is unable to span the membrane. The L156R mutant has ATPase activity,[99)] because the $\alpha_3\beta_3$ complex portion of F_1 is intact, and increased proton permeability through the defective F_o cannot maintain $\Delta\mu H^+$ to inhibit ATP-driven H^+ translocation (*i.e.*, uncoupling).[3),46)]

8.1. Coordination of nuclear and mitochondrial DNA. The tissue activity of F_oF_1 mainly relies on mitochondrial biogenesis encoded by both nDNA and mtDNA (Fig. 9). A number of transcriptional modulators have been implicated in the regulation of mitochondrial biogenesis and oxphos activity.[84)–89)] To understand the nDNA–mtDNA interactions in human cells, we identified the nuclear transcription factors that are common to the expression of these gene products. As Tfam encoded by nDNA is essential for both the initiation of transcription and the replication of mtDNA, we cloned and sequenced the human Tfam gene.[95)] There were sequences in the 5′-upstream regulatory region of Tfam common to those in $HF_1\beta$.[95)] In the absence of mtDNA-coded F_o subunits, expression of other F_oF_1 subunits was not affected, but most nDNA-coded subunits other than α and β of F_oF_1 could not be assembled.[87),96)] For *in vivo* analysis of this regulation, transmitochondrial mice carrying various proportions of deletion mutant mtDNA (ΔmtDNA) were generated by introducing ΔmtDNA from cultured cells into the fertilized eggs of mice.[100)] The great advantage of transmitochon-

drial mice is that they share exactly the same nDNA background and their genetic variations are restricted to the proportions of pathogenic mtDNA.[100]

Transcription factors in the expression of HF_oF_1 include PPARγ coactivator 1α (PGC-1α), in cooperation with several factors, such as peroxisome proliferator-activated receptor (PPAR), nuclear respiratory factors 1 and 2 (NRF-1 and NRF-2), or the specificity protein 1 (Sp1), a ubiquitous transcription factor known to regulate the constitutive expression of oxphos genes (Fig. 10, upper).[86] PGC-1α is a master modulator of gene expression in human tissues and enhances the activity of PPARα in skeletal muscle.[101] Mitochondrial transcription is directed by a small number of nucleus-encoded factors, including Tfam.[95] Expression of these factors is coordinated with that of nuclear respiratory proteins through the action of PGC-1 family coactivators.[101]

Using these cytological methods (Fig. 8), transcriptomics and proteomics (Fig. 9), human bioenergetics at both cell level (Fig. 10) and *in vivo* levels were elucidated.

9. Supramolecular structure of HF_oF_1: Dimeric HF_oF_1, ATP synthasome and ecto-HF_oF_1

Mitochondrial F_oF_1, including HF_oF_1, is typically isolated as a monomeric complex that contains 16 protein subunits[21] and the natural inhibitor protein (IF_1) (Fig. 2).[78] However, mitochondrial F_oF_1 was isolated in dimeric and higher oligomeric states using digitonin for one step mild solubilization followed by blue native (BN) or clear native (CN) electrophoresis.[102] Recent developments in proteomics have revealed HF_oF_1 in its natural supramolecular state.[30),31),102] Single bands in the gel can be analyzed by proteomics approaches including immunoprecipitation,[103] and mass spectrometry to identify the amino acid sequence of the components.[103] Electron microscopy of these oligomeric mitochondrial F_oF_1 particles was reported in 1972 (Fig. 2C in Ref. 3). Dimeric and trimeric F_oF_1 were purified from mammalian mitochondria in five different tissues by BN electrophoresis and CN electrophoresis,[30),102] and these were active, thus suggesting that oligomeric F_oF_1 is constitutive in mitochondria. Using BN electrophoresis, two membrane proteins (6.8 kDa proteolipid and diabetes-associated protein) that had previously been removed during purification were shown to be stoichiometrically associated with F_oF_1,[30] and this may provide insight for further functional investigations.[30]

In situ mitochondrial $\Delta\mu H^+$ was directly estimated by rhodamine 123, which is accumulated in mitochondria depending on $\Delta\mu H^+$.[103] The futile ATP hydrolytic activity of HF_oF_1 during ischemia that lowers $\Delta\mu H^+$, is prevented by IF_1.[78] Bovine IF_1 is an α-helical dimer and residues 1–37 of IF_1 open the catalytic interface between α_D–β_D.[78] Atomic force microscopy images show how these F_oF_1 molecules form dimers with a characteristic 15-nm distance between the axes of their rotors through stereo-specific interactions of the membrane-embedded portions of their stators.[104] A different interaction surface is responsible for the formation of rows of oligomers, suggesting the role of subunits e and g of HF_o in dimerization.[104] Some dimers have a different morphology, with a 10-nm stalk-to-stalk distance, in line with F_oF_1s, which are thus accessible to IF_1.[104] Dimeric or polymeric HF_oF_1 is related to morphology of cristae[104] under the influence of OPA1.[98]

A channel protein, porin, is now known as VDAC (voltage-dependent anion channel) and is the most abundant protein in the mitochondrial outer membrane.[52] VDAC helps ATP/ADP exchange by forming a complex with ANC (ANC–VDAC complex).[103] Finally, a supramolecular structure called ATP synthasome composed of F_oF_1, ANC, PIC and perhaps VDAC was isolated and characterized (Fig. 2).[31] Parallel immuno-electron microscopic studies revealed the presence of PIC and ANC located non-centrally in the basepiece, and other studies indicated an ATP synthase/PIC/ANC stoichiometry near 1:1:1 (Fig. 2).[31] Collectively, these findings support a mechanism in which the entry of the substrates ADP and Pi into mitochondria, the synthesis of ATP on HF_oF_1, and the release and exit of ATP are localized in a supramolecular structure in a highly coordinated system.

9.1. Ectopic HF_oF_1: plasma membrane localization in lipid rafts. HF_oF_1 is located not only on the mitochondrial inner membrane, but also on the cell surface. Extracellular ATP synthesized by the ectopic HF_oF_1 is not an energy source but a regulator for various cellular responses that are initiated by purinergic receptors (P2X and P2Y) and signaling processes and are terminated by breakdown of ATP by ectonucleotidases (Fig. 10, right). By using ^{3}H-ADP, net ^{3}H-ATP synthesis by cell surface HF_oF_1 was confirmed (to rule out ATP + AMP synthesis by adenylate kinase). ATP synthesis was inhibited by membrane-impermeable HF_oF_1-specific inhibitors (angiostatin and piceatannol) and anti-HF_1 anti-

body.[105] Immunoprecipitation indicated that ectopic HF_oF_1 and a surface protein of endothelial cells, caveolin-1, are physically associated.[105] Adipocyte ectopic HF_oF_1 may contain F_o, as it is inhibited by oligomycin and influenced by a proton conductor (uncoupler) (quoted in Ref. 92). HF_oF_1 is selectively localized in lipid rafts with other mitochondrial proteins. Lipid rafts are detergent-resistant membrane microdomains enriched in cholesterol and caveolin-1. Intracellular traffic may translocate HF_oF_1 containing α, β, γ, b, d, F6 and OSCP from mitochondria to lipid rafts.[92]

The ectopic HF_oF_1 has been implicated in numerous activities, including the mediation of intracellular pH, cellular response to antiangiogenic agents, and cholesterol homeostasis as a receptor for apolipoprotein A-1.[106] HF_oF_1 is expressed on the surface of endothelial cells, where it binds angiostatin, regulates surface ATP levels, and modulates endothelial cell proliferation and differentiation *via* purinergic receptor (Fig. 10, right).[106]

Ectopic HF_oF_1 is closely related to obesity.[107] Expression of the α subunit of ectopic HF_oF_1 is markedly increased during adipocyte differentiation. Treatment of differentiated adipocytes with inhibitors of HF_oF_1 or antibodies against α and β subunits of HF_oF_1 leads to a decrease in cytosolic lipid accumulation.[107] Apolipoprotein A-I binds to the β subunit of ectopic HF_oF_1 and its inhibition decreases the production of lipid droplets.[107] Depletion of plasma membrane cholesterol with methyl-beta-cyclodextrin disrupts lipid rafts and abolishes co-localization of HF_oF_1 with caveolin-1, which results in a marked reduction in shear stress-induced ATP release.[105] Endothelial cells release ATP from ectopic HF_oF_1 in response to shear stress, a mechanical force generated by blood flow, and the ATP released modulates cell functions through activation of downstream signals to purinergic receptors.[105] These results suggest that the localization and targeting of HF_oF_1 to caveolin-1/lipid rafts is critical for shear stress-induced ATP release by endothelial cells.[105]

It remains uncertain how F_o components encoded by mtDNA are translocated to rafts as ectopic HF_oF_1, particularly in the form of intact HF_oF_1 (Fig. 10, right). However, inter-organellar traffic of mitochondrial proteins was clearly demonstrated using green fluorescent protein.[103] These mitochondrial dynamics will be discussed in the final section. The energy source ($\Delta\mu H^+$) to synthesize ATP by ectopic HF_oF_1 may not be respiration, but the K^+channel dependent resting potential of plasma membrane is inside negative. These ectopic F_oF_1 activities have never been reported in prokaryotic F_oF_1, although F_oF_1-like V-type ATPase is widely distributed in prokaryotic and mammalian membrane structures to transport ions.[65),68] In mammalian tissues, some proteins involved in energy metabolism may exert entirely different functions; cytochrome c, for example, is an electron carrier but also serves as the central signal protein in apoptosis.

10. *In vivo* ATP synthesis: F_oF_1 in human bioenergetics and diseases

The function and survival of all organisms is dependent on the dynamic control of energy metabolism. Energy demand is matched to ATP supply by F_oF_1 and glycolysis (Fig. 10, bottom).[7),21] The increase in ADP + Pi produced by ATP consumption results in the instant $\Delta\mu H^+$-driven ATP synthesis by F_oF_1 and increases in electron transport activity to compensate $\Delta\mu H^+$ (respiratory control). The increase in ADP is amplified as AMP increase by myokinase reaction (2ADP = ATP + AMP). If ATP synthesis by F_oF_1 is not enough, especially when oxygen supply is limited by high metabolic equivalents (METs >5), increased AMP/ATP ratio activates phosphofructokinase to compensate ATP by glycolysis. Although the regulatory mechanism of TF_oF_1 is basically ubiquitous,[7),108] HF_oF_1 is specialized for human activity. One of the characteristics of HF_oF_1 among other F_oF_1s is genetic polymorphisms during evolution, particularly in mtDNA,[87),109] that cause ethnic and interindividual differences in physical activity, aging and disease susceptibility.[87),109] Voluntary will of the brain triggers muscle contraction and other organ specific activities that consume about 50 kg of ATP per day, but METs change from 0.9 to 15 in a normal adult (Fig. 10, right). Direct measurement of *in vivo* HF_oF_1 activity and AMP/ATP ratio is possible by using ^{31}P magnetic resonance spectroscopy revealed that ATP synthase flux correlated with O_2 uptake (METs) and insulin sensitivity.[110] The increase in METs is mainly caused by actomyosin contraction (Fig. 10, right), and muscle-specific γ subunit splice variants of HF_oF_1 are seen during myogenesis and cardiogenesis (Fig. 7).[32),90] The resulting change in substrates to increase lactic acid can be assessed by ^1H magnetic resonance spectroscopy.[110] Lactic acidemia is present not only in individuals undergoing high MET exercise, but also in the majority of patients with

mitochondrial disorders, including impaired HF_o, and cells isolated from such patients, similarly to ρ^0 cells, require glucose medium (Fig. 8).[22),87)] Mitochondrial disorders can be due to defects in nDNA directly affecting the assembly or function of HF_oF_1 and respiratory chain, defects in mtDNA affecting HF_o and the respiratory chain or nDNA influencing mtDNA structure and viability.[21),87)]

The regulatory mechanism of HF_oF_1 including four independent inhibitory sites[111)] are more complex than those of TF_oF_1.[7),108)] AMP-activated protein kinase (AMPK) activates both oxphos and glycolysis, functioning as a 'fuel gauge' to monitor AMP/ATP ratio (Fig. 10, left).[112)] ATP-sensitive K^+ channels both in the plasma membrane and in mitochondria also monitors ATP levels to regulate cellular activities.[87),113)] Increases in ATP concentration close the K^+ channel, and the resulting depolarization opens L-type Ca^{2+} channels (Fig. 10, bottom). Increased intracellular Ca^{2+} activates many metabolic processes and proteins for mitochondrial dynamics and secretion. For example, in the β-cells of mitochondrial myopathy, ATP-sensitive K^+ channels are not closed and defective Ca^{2+}-dependent insulin secretion results in mitochondrial diabetes.[87)] Mitochondrial ATP-sensitive K^+ channels regulate energy transfer through their regulation of intermembrane space volume and are accordingly essential for the inotropic response during periods of high METs.[113)] Although the target residues in HF_oF_1 and their signal routes have not yet been determined, mitochondrial ATP-sensitive K^+ channels are closely related to kinases including protein kinase Cε.[113)] In fact, detailed proteomics have revealed, for example, phosphorylation of αS76, βT213, βS529, γY44 or γY52, and acetylation of αK132, βK133, γK79 in mammalian F_oF_1.[91)] The monomeric form of HF_oF_1 contains a phosphorylated γ (γY52) that is not present in the dimeric form.[91)]

In contrast to bacteria, ATP synthesis by HF_oF_1 requires exchange of $Pi + ADP$ and ATP between cytosol and mitochondria by PIC and ANC, which are organized as the ATP synthasome (Fig. 2).[31)] VDAC[52)] forming a complex with ANC also plays an important role in cytoplasma-mitocondrial communication.[103)] As mammalian cells are about 1000 times as large as bacteria, and a mitochondrion is as large as a bacterium, mitochondrial dynamics are essential to distribute synthesized ATP (Fig. 10, upper left).[114)] The concept of mitochondrial dynamics includes the movement of mitochondria along the cytoskeleton, the regulation of mitochondrial morphology and distribution, and connectivity mediated by tethering and fusion/fission events.[114)] The relevance of these events in HF_oF_1 activity has been unraveled after the identification of mitofusin[87)] and OPA1.[98)] Subjects with diabetes showed reduced expression (by 26%) of mitofusin 2 and a 39% reduction in the α-subunit of F_oF_1.[115)] Chronic exercise led to increases in VDAC, and the α-subunit of F_oF_1 in muscle from control subjects and from those with diabetes.[115)] Acute exercise caused a 4-fold increase in PGC-1α expression in muscle from control subjects, but not in those with diabetes.[115)]

10.1. Inhibition of HF_oF_1 activity and diseases related to bioenergetics. In the energy metabolism of whole human body,[114),116)] if $\Delta\mu H^+$ is too low, ATP production by HF_oF_1 cannot meet demand (mitochondrial diseases),[22),87)] and if it is too high, reactive oxygen species (ROS) are produced.[23),89),116)] Oxphos is linked to disease through a lack of energy, excess ROS production, or a combination of both,[89),116)] and diseases caused by mitochondrial dysfunction include diabetes, cancer, neurodegenerative disorders and ischemia-reperfusion injury.[23),89),116)]

Because of its complex structure, HF_oF_1 is inhibited by over 250 natural and synthetic inhibitors.[117)] In the absence of torque-driving energy, HF_oF_1 switches from an ATP synthase to an ATP hydrolase, and this occurs during myocardial ischemia. The degree of ATP inefficiently hydrolyzed during ischemia may be as high as 50–90%.[118)] At the start of F_oF_1 study, oligomycin was shown to inhibit F_o,[3),39)–42)] and this portion of F_oF_1 was therefore designated "oligomycin sensitivity conferring factor". Oligomycin cannot be used to treat myocardial ischemia, as it would reduce ATP synthesis in normal tissue.[3)] Only when cellular pH is decreased below 6.8 under ischemia, IF_1[78)] inhibits ATPase at the $\alpha\beta$ interface of HF_1.[78)] The restoration of $\Delta\mu H^+$ favoring ATP synthesis displaces IF_1 from the $\alpha\beta$ interface. However, IF_1 does not completely block hydrolase activity. BMS-199264 selectively inhibits ATPase activity during ischemia while having no effect on ATP synthesis, and enhances the recovery of contractile function following reperfusion.[118)] IF_1, ectopic HF_oF_1 and the opener of mitochondrial ATP-sensitive K^+ channel[113)] protect cardiomyocytes from ischemic/reperfusion damage.

As HF_oF_1 supplies most ATP needed for human activity, further study will provide useful insight for

emergency medicine,[118] mitochondrial cardiomyopathy[22),87] and obesity-related chronic diseases.[23),115),116]

Conclusions

The excellent work to date on ATP synthases (F_oF_1) has been reviewed based on data obtained in studies on TF_oF_1 and HF_oF_1. The chemiosmotic theory[1] was firmly established by $\Delta\mu H^+$-driven ATP synthesis in TF_oF_1 liposomes (Figs. 1 and 3),[7),46] and the rotational theory[4] was established by crucial observations of γ-rotation[10),11),17] and ATP synthesis on externally added torque to rotate γ in TF_1 (Fig. 1).[64] TF_1 is the only F_1 sufficiently stable to be consistently analyzed by reconstitution, crystallography, mutagenesis, and nanotechnology for torque-driven ATP synthesis.[7] Crystallographic analysis using BF_1 (Figs. 2 and 5)[9),25] and TF_1 (Figs. 4–6),[71),74] site-directed mutagenesis using EF_oF_1[18),65] and TF_oF_1 (Figs. 5 and 6),[12),20),63] and dynamic nanotechnology[79] have contributed to elucidating elastic[7),74] and loose[61] energy coupling. Based on the fundamental mechanism of ATP synthesis in TF_oF_1,[7),108] and functional complementation of YF_1-deleted yeast with BF_1 genes,[8] human bioenergetics was developed by research on HF_oF_1 using plasmids,[21),28),86),97] transgenic mice (Fig. 7),[23),90),100] cytoplasts (Fig. 8)[33),87] and omics (Fig. 9).[21),84),86),87] HF_oF_1 differed from TF_oF_1 in complex structure (Fig. 2), mitochondrial genetics (Fig. 8),[87] organ specificity (Fig. 7)[90] and intricate biogenesis (Fig. 9).[86] The complex regulation of HF_oF_1 has been shown to be essential for daily human activity that is triggered by the brain (Fig. 10), thus human bioenergetics is also applicable to emergency medicine[113),118] and obesity/diabetes[23),116] and mitochondrial diseases.[87),97]

Acknowledgments

The author extends thanks to Profs. M. Yoshida, T. Hamamoto, H. Endo, S. Ohta, E. Muneyuki, H. Hirata, M. Yohda and N. Sone, with whom he has worked in the Department of Biochemistry, Jichi Medical School since 1972, for their excellent work. The author would also like to thank Prof. E. Racker for his excellent advice. This study was supported by several Grants-in-Aid (1973–2008), and the "High-Tech Research Center" Project for Private Universities matching fund subsidy (1999–2008; for Y.K.) from the Ministry of Education, Culture, Sports, Science and Technology of Japan.

References

1) Mitchell, P. (1961) Coupling of phosphorylation to electron and hydrogen transfer by a chemiosmotic type of mechanism. Nature **191**, 144–148.
2) Pullman, M.E., Penefsky, H.S., Datta, A. and Racker, E. (1960) Partial resolution of the enzymes catalyzing oxidative phosphorylation. I. Purification and properties of soluble, dinitrophenol-stimulated adenosine triphosphatase. J. Biol. Chem. **235**, 3322–3329.
3) Kagawa, Y. (1972) Reconstitution of oxidative phosphorylation. Biochim. Biophys. Acta **265**, 297–338.
4) Boyer, P.D. (1997) The ATP synthase-a splendid molecular machine. Annu. Rev. Biochem. **66**, 717–749.
5) Yoshida, M., Sone, N., Hirata, H., Kagawa, Y. and Ui, N. (1979) Subunit structure of adenosine triphosphatase. Comparison of the structure in thermophilic bacterium PS3 with those in mitochondria, chloroplasts, and *Escherichia coli*. J. Biol. Chem. **254**, 9525–9533.
6) Ohta, S., Tsuboi, M., Oshima, T., Yoshida, M. and Kagawa, Y. (1980) Nucleotide binding to isolated alpha and beta subunits of proton-translocating adenosine triphosphatase with circular dichroism. J. Biochem. **87**, 1609–1617.
7) Kagawa, Y. (1999) Biophysical studies on ATP synthase. Adv. Biophys. **36**, 1–25.
8) Puri, N., Lai-Zhang, J., Meier, S. and Mueller, D.M. (2005) Expression of bovine F_1-ATPase with functional complementation in yeast *Saccharomyces cerevisiae*. J. Biol. Chem. **280**, 22418–22424.
9) Abrahams, J.P., Leslie, A.G., Lutter, R. and Walker, J.E. (1994) Structure at 2.8 A resolution of F_1-ATPase from bovine heart mitochondria. Nature **370**, 621–628.
10) Kagawa, Y. and Hamamoto, T. (1996) The energy transmission in ATP synthase: from the γ-c rotor to the $\alpha_3\beta_3$ oligomer fixed by OSCP-b stator via the βDELSEED sequence. J. Bioenerg. Biomembr. **28**, 421–431.
11) Noji, H., Yasuda, R., Yoshida, M. and Kinosita, K. Jr. (1997) Direct observation of the rotation of F_1-ATPase. Nature **386**, 299–302.
12) Ohta, S., Yohda, M., Ishizuka, M., Hirata, H., Hamamoto, T., Otawara-Hamamoto, Y. *et al.* (1988) Sequence and over-expression of subunits of adenosine triphosphate synthase in thermophilic bacterium PS3. Biochim. Biophys. Acta **933**, 141–155.
13) Sambongi, Y., Iko, Y., Tanabe, M., Omote, H., Iwamoto-Kihara, A., Ueda, I. *et al.* (1999) Mechanical rotation of the c subunit oligomer in ATP synthase (F_0F_1): direct observation. Science **286**, 1722–1724.
14) Stock, D., Leslie, A.G.W. and Walker, J.E. (1999) Molecular architecture of the rotary motor in ATP synthase. Science **286**, 1700–1705.
15) Mitome, N., Suzuki, T., Hayashi, S. and Yoshida,

M. (2004) Thermophilic ATP synthase has a decamer c-ring: indication of noninteger 10:3 H^+/ATP ratio and permissive elastic coupling. Proc. Natl. Acad. Sci. USA **101**, 12159–12164.
16) Düser, M.G., Zarrabi, N., Cipriano, D.J., Ernst, S., Glick, G.D., Dunn, S.D. *et al.* (2009) 36° step size of proton-driven c-ring rotation in F_oF_1-ATP synthase. EMBO J. **28**, 2689–2696.
17) Yoshida, M., Muneyuki, E. and Hisabori, T. (2001) ATP synthase—a marvelous rotary engine of the cell. Nat. Rev. Mol. Cell Biol. **2**, 669–677.
18) Futai, M., Noumi, T. and Maeda, M. (1989) ATP synthase (H^+-ATPase): results by combined biochemical and molecular biological approaches. Annu. Rev. Biochem. **58**, 111–136.
19) Kagawa, Y., Ishizuka, M., Saishu, T. and Nakao, S. (1986) Stable structure of thermophilic proton ATPase beta subunit. J. Biochem. **100**, 923–934.
20) Yohda, M., Ohta, S., Hisabori, T. and Kagawa, Y. (1988) Site-directed mutagenesis of stable adenosine triphosphate synthase. Biochim. Biophys. Acta **933**, 156–164.
21) Kagawa, Y., Hamamoto, T., Endo, H., Ichida, M., Shibui, H. and Hayakawa, M. (1997) Genes of human ATP synthase: Their roles in physiology and aging. Biosci. Rep. **17**, 115–146.
22) Isobe, K., Ito, S., Hosaka, H., Iwamura, Y., Kondo, H., Kagawa, Y. *et al.* (1998) Nuclear-recessive mutations of factors involved in mitochondrial translation are responsible for age-related respiration deficiency of human skin fibroblasts. J. Biol. Chem. **273**, 4601–4606.
23) Kagawa, Y., Yanagisawa, Y., Hasegawa, K., Suzuki, H., Yasuda, K., Kudo, H. *et al.* (2002) Single nucleotide polymorphism of thrifty genes for energy metabolism: evolutionary origins and prospects for intervention to prevent obesity-related diseases. Biochem. Biophys. Res. Commun. **295**, 207–222.
24) Walker, J.E., Fearnley, I.M., Gay, N.J., Gibson, B.W., Northrop, F.D., Powell, S. *et al.* (1985) Primary structure and subunit stoichiometry of F_1-ATPase from bovine mitochondria. J. Mol. Biol. **184**, 677–701.
25) Walker, J.E. and Dickson, V.K. (2006) The peripheral stalk of the mitochondrial ATP synthase. Biochim. Biophys. Acta **1757**, 286–296.
26) Anderson, S., Bankier, A.T., Barrell, B.G., de Bruijn, M.H., Coulson, A.R., Drouin, J. *et al.* (1981) Sequence and organization of the human mitochondrial genome. Nature **290**, 457–465.
27) Matsuda, C., Endo, H., Ohta, S. and Kagawa, Y. (1993) Gene structure of human mitochondrial ATP synthase gamma-subunit. Tissue specificity produced by alternative RNA splicing. J. Biol. Chem. **268**, 24950–24958.
28) Ohta, S., Tomura, H., Matsuda, K. and Kagawa, Y. (1988) Gene structure of the human mitochondrial adenosine triphosphate synthase beta subunit. J. Biol. Chem. **263**, 11257–11262.
29) Gibbons, C., Montgomery, M.G., Leslie, A.G. and Walker, J.E. (2000) The structure of the central stalk in bovine F_1-ATPase at 2.4 A resolution. Nat. Struct. Biol. **7**, 1055–1061.
30) Krause, F., Reifschneider, N.H., Goto, S. and Dencher, N.A. (2005) Active oligomeric ATP synthases in mammalian mitochondria. Biochem. Biophys. Res. Commun. **329**, 583–590.
31) Chen, C., Ko, Y., Delannoy, M., Ludtke, S.J., Chiu, W. and Pedersen, P.L. (2004) Mitochondrial ATP synthasome: three-dimensional structure by electron microscopy of the ATP synthase in complex formation with carriers for Pi and ADP/ATP. J. Biol. Chem. **279**, 31761–31768.
32) Ichida, M., Hakamata, Y., Hayakawa, M., Ueno, E., Ikeda, U., Shimada, K. *et al.* (2000) Differential regulation of exonic regulatory elements for muscle-specific alternative splicing during myogenesis and cardiogenesis. J. Biol. Chem. **275**, 15992–16001.
33) Hayashi, J., Ohta, S., Kagawa, Y., Kondo, H., Kaneda, H., Yonekawa, H. *et al.* (1994) Nuclear but not mitochondrial genome involvement in human age-related mitochondrial dysfunction. Functional integrity of mitochondrial DNA from aged subjects. J. Biol. Chem. **269**, 6878–6883.
34) Fleischer, S., Brierley, G., Klouwen, H. and Slautterback, D.B. (1962) Studies of the electron transfer system. XLVII. The role of phospholipids in electron transfer. J. Biol. Chem. **237**, 3264–3272.
35) Kakiuchi, S. (1927) The significance of lipoids in the oxygen consuming activity of tissues. 1. The oxygen consuming activity of tissue and the mitochondrial structure. J. Biochem. **7**, 263–265.
36) Okunuki, K. (1940) Ueber die Rolle der Diaphorase in der Wechsel-wirkung zwischen dem Cytochrom b und dem Dehydrasesystem. Proc. Imp. Acad. (Tokyo) **16**, 144–148.
37) Green, D.E. and Hatefi, Y. (1961) The mitochondrion and biochemical machines. Science **133**, 13–19.
38) Small, D.M., Bourges, M.C. and Dervichian, D.G. (1966) The biophysics of lipidic associates I. The ternary systems lecithin-bile salt-water. Biochim. Biophys. Acta **125**, 563–581.
39) Kagawa, Y. and Racker, E. (1971) Partial resolution of the enzymes catalyzing oxidative phosphorylation. XXV. Reconstitution of vesicles catalyzing ^{32}Pi-adenosine triphosphate exchange. J. Biol. Chem. **246**, 5477–5487.
40) Kagawa, Y., Kandrach, A. and Racker, E. (1973) Partial resolution of the enzymes catalyzing oxidative phosphorylation. XXVI. Specificity of phospholipids required for energy transfer reactions. J. Biol. Chem. **248**, 676–684.
41) Kagawa, Y. and Racker, E. (1966) Partial resolution of the enzymes catalyzing oxidative phosphorylation. VIII. Properties of a factor conferring oligomycin sensitivity on mitochondrial adenosine triphosphatase. J. Biol. Chem. **241**, 2461–2466.
42) Kagawa, Y. and Racker, E. (1966) Partial resolution of the enzymes catalyzing oxidative phosphorylation. IX. Reconstruction of oligomycin-sensitive

adenosine triphosphatase. J. Biol. Chem. **241**, 2467–2474.
43) Kagawa, Y. and Racker, E. (1966) Partial resolution of the enzymes catalyzing oxidative phosphorylation. X. Correlation of morphology and function in submitochondrial particles. J. Biol. Chem. **241**, 2475–2482.
44) Yoshida, M., Sone, N., Hirata, H. and Kagawa, Y. (1975) A highly stable adenosine triphosphatase from a thermophilic bacterium. Purification, properties and reconstitution. J. Biol. Chem. **250**, 7910–7916.
45) Sone, N., Yoshida, M., Hirata, H. and Kagawa, Y. (1975) Purification, properties of a dicyclohexylcarbodiimide-sensitive adenosine triphosphatase from a thermophilic bacterium. J. Biol. Chem. **250**, 7917–7923.
46) Sone, N., Yoshida, M., Hirata, H. and Kagawa, Y. (1977) Adenosine triphosphate synthesis by electrochemical proton gradient in vesicles reconstituted from purified adenosine triphosphatase and phospholipids of thermophilic bacterium. J. Biol. Chem. **252**, 2956–2960.
47) Jagendorf, A.T. (1967) Acid-base transitions and phosphorylation by chloroplasts. Fed. Proc. **26**, 1361–1369.
48) Witt, H.T., Schlodder, E. and Gräber, P. (1976) Membrane-bound ATP synthesis generated by an external electrical field. FEBS Lett. **69**, 272–276.
49) Okamoto, H., Sone, N., Hirata, H., Yoshida, M. and Kagawa, Y. (1977) Purified proton conductor in proton translocating adenosine triphosphatase of a thermophilic bacterium. J. Biol. Chem. **252**, 6125–6131.
50) Rögner, M., Ohno, K., Hamamoto, T., Sone, N. and Kagawa, Y. (1979) Net ATP synthesis in H^+-ATPase macroliposomes by an external electric field. Biochem. Biophys. Res. Commun. **91**, 362–367.
51) Muneyuki, E., Kagawa, Y. and Hirata, H. (1989) Steady state kinetics of proton translocation catalyzed by thermophilic F_oF_1-ATPase reconstituted in planar bilayer membranes. J. Biol. Chem. **264**, 6092–6096.
52) Zalman, L.S., Nikaido, H. and Kagawa, Y. (1980) Mitochondrial outer membrane contains a protein producing nonspecific diffusion channels. J. Biol. Chem. **255**, 1771–1774.
53) Yoshida, M., Sone, N., Hirata, H. and Kagawa, Y. (1977) Reconstitution of adenosine triphosphatase of thermophilic bacterium from purified individual subunits. J. Biol. Chem. **252**, 3480–3485.
54) Kagawa, Y. and Hamamoto, T. (1997) Intramolecular rotation in ATP synthase: dynamic and crystallographic studies on thermophilic F_1. Biochem. Biophys. Res. Commun. **240**, 247–256.
55) Kagawa, Y., Ohta, S., Harada, M., Sato, M. and Itoh, Y. (1992) The $\alpha_3\beta_3$ and $\alpha_1\beta_1$ complexes of ATP synthase. Ann. N. Y. Acad. Sci. **671**, 366–376.
56) Yagi, H., Kajiwara, N., Iwabuchi, T., Izumi, K., Yoshida, M. and Akutsu, H. (2009) Stepwise propagation of the ATP-induced conformational change of the F_1-ATPase β subunit revealed by NMR. J. Biol. Chem. **284**, 2374–2382.
57) Saika, K. and Yoshida, M. (1995) A minimum catalytic unit of F_1-ATPase shows non-cooperative ATPase activity inherent in a single catalytic site with a Km 70 µM. FEBS Lett. **368**, 207–210.
58) Miwa, K. and Yoshida, M. (1989) The $\alpha_3\beta_3$ complex, the catalytic core of F_1-ATPase. Proc. Natl. Acad. Sci. USA **86**, 6484–6487.
59) Paik, S.R., Yokoyama, K., Yoshida, M., Ohta, T., Kagawa, Y. and Allison, W.S. (1993) The TF_1-ATPase and ATPase activities of assembled $\alpha_3\beta_3\gamma$, $\alpha_3\beta_3\gamma\delta$, and $\alpha_3\beta_3\gamma\varepsilon$ complexes are stimulated by low and inhibited by high concentrations of rhodamine 6G whereas the dye only inhibits the $\alpha_3\beta_3$, and $\alpha_3\beta_3\delta$ complexes. J. Bioenerg. Biomembr. **25**, 679–684.
60) Aloise, P., Kagawa, Y. and Coleman, P.S. (1991) Comparative Mg^{2+}-dependent sequential covalent binding stoichiometries of 3′-O-(4-benzoyl)benzoyl adenosine 5′-diphosphate of MF_1, TF_1, and the $\alpha3\beta3$ core complex of TF_1. The binding change motif is independent of the F_1 $\gamma\delta\varepsilon$ subunits. J. Biol. Chem. **266**, 10368–10376.
61) Oosawa, F. and Hayashi, S. (1986) The loose coupling mechanism in molecular machines of living cells. Adv. Biophys. **22**, 151–183.
62) Feniouk, B.A. and Yoshida, M. (2007) Regulatory mechanisms of proton-translocating F_oF_1-ATP synthase. Results Probl. Cell Differ. **45**, 279–308.
63) Ariga, T., Muneyuki, E. and Yoshida, M. (2007) F_1-ATPase rotates by an asymmetric, sequential mechanism using all three catalytic subunits. Nat. Struct. Mol. Biol. **14**, 841–846.
64) Itoh, H., Takahashi, A., Adachi, K., Noji, H., Yasuda, R., Yoshida, M. *et al.* (2004) Mechanically driven ATP synthesis by F_1-ATPase. Nature **427**, 465–468.
65) Futai, M., Wada, Y. and Kaplan, J.H. (eds.) (2004) Handbook of ATPases. Wiley-VCH, Germany. pp. 1–468.
66) Kagawa, Y., Nojima, H., Nukiwa, N., Ishizuka, M., Nakajima, T., Yasuhara, T. *et al.* (1984) High guanine plus cytosine content in the third letter of codons of an extreme thermophile. DNA sequence of the isopropylmalate dehydrogenase of *Thermus thermophilus*. J. Biol. Chem. **259**, 2956–2960.
67) Ohtsubo, M., Yoshida, M., Ohta, S., Kagawa, Y., Yohda, M. and Date, T. (1987) *In vitro* mutated β subunits from the F_1-ATPase of the thermophilic bacterium, PS3, containing glutamine in place of glutamic acid in positions 190 or 201 assembles with the α and γ subunits to produce inactive complexes. Biochem. Biophys. Res. Commun. **146**, 705–710.
68) Imamura, H., Nakano, M., Noji, H., Muneyuki, E., Ohkuma, S., Yoshida, M. *et al.* (2003) Evidence for rotation of V_1-ATPase. Proc. Natl. Acad. Sci. USA **100**, 2312–2315.
69) Wakabayashi, T., Kubota, M., Yoshida, M. and Kagawa, Y. (1977) Structure of ATPase (coupling

factor TF_1) from a thermophilic bacterium. J. Mol. Biol. **117**, 515–519.
70) Shirakihara, Y., Yohda, M., Kagawa, Y., Yokoyama, K. and Yoshida, M. (1991) Purification by dye-ligand chromatography and a crystallization study of the F_1-ATPase and its major subunits, β and α, from a thermophilic bacterium, PS3. J. Biochem. **109**, 466–471.
71) Shirakihara, Y., Leslie, A.G., Abrahams, J.P., Walker, J.E., Ueda, T., Sekimoto, Y. *et al.* (1997) The crystal structure of the nucleotide-free $\alpha_3\beta_3$ subcomplex of F_1-ATPase from the thermophilic *Bacillus* PS3 is a symmetric trimer. Structure **5**, 825–836.
72) Vollmar, M., Schlieper, D., Winn, M., Büchner, C. and Groth, G. (2009) Structure of the c14 rotor ring of the proton translocating chloroplast ATP synthase. J. Biol. Chem. **284**, 18228–18235.
73) Dickson, V.K., Silvester, J.A., Fearnley, I.M., Leslie, A.G. and Walker, J.E. (2006) On the structure of the stator of the mitochondrial ATP synthase. EMBO J. **25**, 2911–2918.
74) Kagawa, Y., Hamamoto, T. and Endo, H. (2000) The α/β interfaces of $\alpha_1\beta_1$, $\alpha_3\beta_3$, and F_1: Domain motions and elastic energy stored during γ rotation. J. Bioenerg. Biomembr. **32**, 471–484.
75) Kabaleeswaran, V., Shen, H., Symersky, J., Walker, J.E., Leslie, A.G. and Mueller, D.M. (2009) Asymmetric structure of the yeast F_1 ATPase in the absence of bound nucleotides. J. Biol. Chem. **284**, 10546–10551.
76) Kagawa, R., Montgomery, M.G., Braig, K., Leslie, A.G. and Walker, J.E. (2004) The structure of bovine F_1-ATPase inhibited by ADP and beryllium fluoride. EMBO J. **23**, 2734–2744.
77) Senter, P., Eckstein, F. and Kagawa, Y. (1983) Substrate metal adenosine 5′-triphosphate chelate structure and stereochemical course of reaction catalyzed by the adenosine triphosphatase from the thermophilic bacterium PS3. Biochemistry **22**, 5514–5518.
78) Cabezón, E., Montgomery, M.G., Leslie, A.G. and Walker, J.E. (2003) The structure of bovine F_1-ATPase in complex with its regulatory protein IF_1. Nat. Struct. Biol. **10**, 744–750.
79) Yasuda, R., Masaike, T., Adachi, K., Noji, H., Itoh, H. and Kinosita, K. Jr. (2003) The ATP-waiting conformation of rotating F_1-ATPase revealed by single-pair fluorescence resonance energy transfer. Proc. Natl. Acad. Sci. USA **100**, 9314–9318.
80) Galvez, E.M., Zimmermann, B., Rombach-Riegraf, V., Bienert, R. and Gräber, P. (2007) Fluorescence resonance energy transfer in single enzyme molecules with a quantum dot as donor. Eur. Biophys. J. **37**, 1367–1371.
81) Masaike, T., Koyama-Horibe, F., Oiwa, K., Yoshida, M. and Nishizaka, T. (2008) Cooperative three-step motions in catalytic subunits of F_1-ATPase correlate with 80 degrees and 40 degrees substep rotations. Nat. Struct. Mol. Biol. **15**, 1326–1333.
82) Steigmiller, S., Turina, P. and Gräber, P. (2008) The thermodynamic H^+/ATP ratios of the H^+-ATPsynthases from chloroplasts and *Escherichia coli*. Proc. Natl. Acad. Sci. USA **105**, 3745–3750.
83) Sielaff, H., Rennekamp, H., Wächter, A., Xie, H., Hilbers, F., Feldbauer, K. *et al.* (2008) Domain compliance and elastic power transmission in rotary F_oF_1-ATPase. Proc. Natl. Acad. Sci. USA **105**, 17760–17765.
84) Akiyama, S., Endo, H., Inohara, N., Ohta, S. and Kagawa, Y. (1994) Gene structure and cell type-specific expression of the human ATP synthase alpha subunit. Biochim. Biophys. Acta **1219**, 129–140.
85) Tomura, H., Endo, H., Kagawa, Y. and Ohta, S. (1990) Novel regulatory enhancer in the nuclear gene of the human mitochondrial ATP synthase beta-subunit. J. Biol. Chem. **265**, 6525–6527.
86) Kagawa, Y. and Ohta, S. (1990) Regulation of mitochondrial ATP synthesis in mammalian cells by transcriptional control. Int. J. Biochem. **22**, 219–229.
87) Sato, A., Endo, H., Umetsu, K., Sone, H., Yanagisawa, Y., Saigusa, A. *et al.* (2003) Polymorphism, heteroplasmy, mitochondrial fusion and diabetes. Biosci. Rep. **23**, 313–337.
88) Vives-Bauza, C., Magrane, J., Andreu, A.L. and Manfredi, G. (2010) Novel role of ATPase subunit c targeting peptide beyond mitochondrial import. Mol. Biol. Cell **21**, 131–139.
89) Hüttemann, M., Lee, I., Pecinova, A., Pecina, P., Przyklenk, K. and Doan, J.W. (2008) Regulation of oxidative phosphorylation, the mitochondrial membrane potential, and their role in human disease. J. Bioenerg. Biomembr. **40**, 445–456.
90) Hayakawa, M., Sakashita, E., Ueno, E., Tominaga, S., Hamamoto, T., Kagawa, Y. *et al.* (2002) Muscle-specific exonic splicing silencer for exon exclusion in human ATP synthase gamma-subunit pre-mRNA. J. Biol. Chem. **277**, 6974–6984.
91) Kane, L.A. and Van Eyk, J.E. (2009) Post-translational modifications of ATP synthase in the heart: biology and function. J. Bioenerg. Biomembr. **41**, 145–150.
92) Champagne, E., Martinez, L.O., Collet, X. and Barbaras, R. (2006) Ecto-F_1F_o ATP synthase/F_1 ATPase: metabolic and immunological functions. Curr. Opin. Lipidol. **17**, 279–284.
93) Dillin, A., Hsu, A.L., Arantes-Oliveira, N., Lehrer-Graiwer, J., Hsin, H., Fraser, A.G. *et al.* (2002) Rates of behavior and aging specified by mitochondrial function during development. Science **298**, 2398–2401.
94) Ito, S., Ohta, S., Nishimaki, K., Kagawa, Y., Soma, R., Kuno, S.Y. *et al.* (1999) Functional integrity of mitochondrial genomes in human platelets and autopsied brain tissues from elderly patients with Alzheimer's disease. Proc. Natl. Acad. Sci. USA **95**, 2099–2103.
95) Tominaga, K., Akiyama, S., Kagawa, Y. and Ohta, S. (1992) Upstream region of a genomic gene for human mitochondrial transcription factor 1. Biochim. Biophys. Acta **1131**, 217–219.

96) Smith, C.P. and Thorsness, P.E. (2005) Formation of an energized inner membrane in mitochondria with a gamma-deficient F_1-ATPase. Eukaryot. Cell **4**, 2078–2086.
97) Kagawa, Y. and Hayashi, J.-I. (1997) Gene therapy of mitochondrial diseases using human cytoplasts. Gene Ther. **4**, 6–10.
98) Satoh, M., Hamamoto, T., Seo, N., Kagawa, Y. and Endo, H. (2003) Differential sublocalization of the dynamin-related protein OPA1 isoforms in mitochondria. Biochem. Biophys. Res. Commun. **300**, 482–493.
99) Solaini, G., Harris, D.A., Lenaz, G., Sgarbi, G. and Baracca, A. (2008) The study of the pathogenic mechanism of mitochondrial diseases provides information on basic bioenergetics. Biochim. Biophys. Acta **1777**, 941–945.
100) Nakada, K., Sato, A., Sone, H., Kasahara, A., Ikeda, K., Kagawa, Y. *et al.* (2004) Accumulation of pathogenic DeltamtDNA induced deafness but not diabetic phenotypes in mito-mice. Biochem. Biophys. Res. Commun. **323**, 175–184.
101) Chanséaume, E. and Morio, B. (2009) Potential mechanisms of muscle mitochondrial dysfunction in aging and obesity and cellular consequences. Int. J. Mol. Sci. **10**, 306–324.
102) Meyer, B., Wittig, I., Trifilieff, E., Karas, M. and Schägger, H. (2007) Identification of two proteins associated with mammalian ATP synthase. Mol. Cell. Proteomics **6**, 1690–1699.
103) Kasashima, K., Ohta, E., Kagawa, Y. and Endo, H. (2006) Mitochondrial functions and estrogen receptor-dependent nuclear translocation of pleiotropic human prohibitin 2. J. Biol. Chem. **281**, 36401–36410.
104) Buzhynskyy, N., Sens, P., Prima, V., Sturgis, J.N. and Scheuring, S. (2007) Rows of ATP synthase dimers in native mitochondrial inner membranes. Biophys. J. **93**, 2870–2876.
105) Yamamoto, K., Shimizu, N., Obi, S., Kumagaya, S., Taketani, Y., Kamiya, A. *et al.* (2007) Involvement of cell surface ATP synthase in flow-induced ATP release by vascular endothelial cells. Am. J. Physiol. Heart Circ. Physiol. **293**, H1646–H1653.
106) Chi, S.L. and Pizzo, S.V. (2006) Cell surface F_1F_o ATP synthase: a new paradigm? Ann. Med. **38**, 429–438.
107) Arakaki, N., Kita, T., Shibata, H. and Higuti, T. (2007) Cell-surface H^+-ATP synthase as a potential molecular target for anti-obesity drugs. FEBS Lett. **581**, 3405–3409.
108) von Ballmoos, C., Wiedenmann, A. and Dimroth, P. (2009) Essentials for ATP synthesis by F_1F_0 ATP synthases. Annu. Rev. Biochem. **78**, 649–672.
109) Takasaki, S. (2009) Mitochondrial haplogroups associated with Japanese centenarians, Alzheimer's patients, Parkinson's patients, type 2 diabetic patients and healthy non-obese young males. J. Genet. Genomics **36**, 425–434.
110) Kacerovsky-Bielesz, G., Chmelik, M., Ling, C., Pokan, R., Szendroedi, J., Farukuoye, M. *et al.* (2009) Short-term exercise training does not stimulate skeletal muscle ATP synthesis in relatives of humans with type 2 diabetes. Diabetes **58**, 1333–1341.
111) Gledhill, J.R. and Walker, J.E. (2006) Inhibitors of the catalytic domain of mitochondrial ATP synthase. Biochem. Soc. Trans. **34**, 989–992.
112) Steinberg, G.R. and Kemp, B.E. (2009) AMPK in Health and Disease. Physiol. Rev. **89**, 1025–1078.
113) Costa, A.D. and Garlid, K.D. (2009) MitoKATP activity in healthy and ischemic hearts. J. Bioenerg. Biomembr. **41**, 123–126.
114) Liesa, M., Palacín, M. and Zorzan, A. (2009) Mitochondrial dynamics in mammalian health and disease. Physiol. Rev. **89**, 799–845.
115) Hernández-Alvarez, M.I., Thabit, H., Burns, N., Shah, S., Brema, I., Hatunic, M. *et al.* (2009) Subjects with early-onset type 2 diabetes show defective activation of the skeletal muscle PGC-1α/mitofusin-2 regulatory pathway in response to physical activity. Diabetes Care **33**, 645–651.
116) Kagawa, Y., Cha, S., Hasegawa, K., Hamamoto, T. and Endo, H. (1999) Regulation of energy metabolism in human cells in aging and diabetes: F_oF_1, mtDNA, UCP, and ROS. Biochem. Biophys. Res. Commun. **266**, 662–676.
117) Hong, S. and Pedersen, P.L. (2008) ATP synthase and the actions of inhibitors utilized to study its roles in human health, disease, and other scientific areas. Microbiol. Mol. Biol. Rev. **72**, 590–641.
118) Grover, G.J. and Malm, J. (2008) Pharmacological profile of the selective mitochondrial F_1F_0 ATP hydrolase inhibitor BMS-199264 in myocardial ischemia. Cardiovasc. Ther. **26**, 287–296.

(Received Dec. 23, 2009; accepted Apr. 30, 2010)

Profile

Yasuo Kagawa was born in 1932. He graduated from the Medical School at the University of Tokyo in 1957, and after completing an internship at St. Luke's Hospital, he received his PhD from the Graduate School of the University of Tokyo in 1962. He continued his bioenergetics research as a Fulbright scholar at the Public Health Research Institute of New York in 1963, as an assistant at the University of Tokyo in 1965, as a professor at Shinshu University in 1968, as a visiting professor of Biochemistry and Molecular Biology at Cornell University in 1970, and, since 1972, as a professor at Jichi Medical School (JMS), where his studies on F_1F_o ATP synthase have garnered international attention. After retiring in 1998, Dr. Kagawa was appointed Professor Emeritus at JMS and joined Kagawa Nutrition University (KNU) as a professor of Medical Chemistry. He became the vice president of KNU in 1999. He has also served as managing editor of several international journals, and was a committee member of the International Union of Biochemistry and Molecular Biology. Dr. Kagawa has received several awards, including the Medical Research Prize from the Japanese Medical Association in 1985, the Medal with Purple Ribbon in 1996, and the Order of the Sacred Treasure, Gold Rays with Neck Ribbon from the Government of Japan in 2006.